



UNIVERSIDAD DE INVESTIGACIÓN DE TECNOLOGÍA EXPERIMENTAL YACHAY

Escuela de Ciencias de la Tierra, Energía y Ambiente

Sequence Stratigraphy of the Northern Part of the Ecuadorian Coastal Basins Combining Seismic and Well Log Data

Trabajo de integración curricular presentado como requisito para la
obtención del título de Geólogo

Autor:

Pijal Morejón Daniel Alexander

Tutor:

M.Sc. Perez Roa Richard

Co-Tutor:

Ph.D. Vázquez-Taset Yaniel

Urcuquí, Septiembre, 2024

Autoría

Yo, **DANIEL ALEXANDER PIJAL MOREJÓN**, con cédula de identidad 1004108542, declaro que las ideas, juicios, valoraciones, interpretaciones, consultas bibliográficas, definiciones y conceptualizaciones expuestas en el presente trabajo; así cómo, los procedimientos y herramientas utilizadas en la investigación, son de absoluta responsabilidad de el/la autor/a del trabajo de integración curricular. Así mismo, me acojo a los reglamentos internos de la Universidad de Investigación de Tecnología Experimental Yachay.

Urququí, Septiembre, 2024.

Daniel Alexander Pijal Morejón

CI:1004108542

Autorización de publicación

Yo, **DANIEL ALEXANDER PIJAL MOREJÓN**, con cédula de identidad 1004108542, cedo a la Universidad de Investigación de Tecnología Experimental Yachay, los derechos de publicación de la presente obra, sin que deba haber un reconocimiento económico por este concepto. Declaro además que el texto del presente trabajo de titulación no podrá ser cedido a ninguna empresa editorial para su publicación u otros fines, sin contar previamente con la autorización escrita de la Universidad.

Asimismo, autorizo a la Universidad que realice la digitalización y publicación de este trabajo de integración curricular en el repositorio virtual, de conformidad a lo dispuesto en el Art. 144 de la Ley Orgánica de Educación

Urcuquí, Septiembre, 2024.

Daniel Alexander Pijal Morejón

CI:1004108542

Dedication

To my family, for their unwavering love, endless patience, and steadfast support, even through the most challenging times. Your resilience and belief in me have been my guiding light, providing strength and encouragement when I needed it most. I am profoundly grateful for every sacrifice you've made on my behalf, which has shaped me into the person I am today. This achievement is not just mine; it is a testament to the enduring love and support that you have generously given me.

Daniel Alexander Pijal Morejón

Acknowledgment

En este camino hacia la culminación de mi carrera universitaria, me embarga una profunda gratitud hacia aquellos cuya presencia ha sido fundamental en mi desarrollo personal y académico. Mi primer y más sentido agradecimiento es para mi familia: a mi madre, Myriam, por su amor y apoyo incondicional que han sido mi refugio y fortaleza; a mi padre, Edwin, quien con su educación y sabiduría me enseñó a enfocar y alcanzar las metas de mi vida; a mi hermano, Santiago, cuyo ejemplo me ha inspirado continuamente; a mi cuñada, Erika, y a mis sobrinos, Benja y Emi, quienes han añadido color a mi vida, haciéndola más hermosa de lo que imaginaba; a David, mi hermano y compañero de vida; y en un lugar especial, mi ángel en el cielo, mi hermano Pato, por quien he cumplido mis promesas y sé que desde arriba me guía y protege. Mis tíos merecen un agradecimiento especial por ser parte esencial de mi entorno familiar; y Ares, por ser mi apoyo emocional.

Un agradecimiento profundo a mis profesores en la Universidad, especialmente a mi tutor, Richard Pérez, y a mi cotutor, Yaniel Vázquez, por su orientación invaluable y por ser ejemplos de dedicación y excelencia.

A mis amigos de siempre, Alejandro, Ruben, Ashley, Danny, Sebastian, y Tito, gracias por acompañarme en cada paso de este viaje, ofreciéndome su amistad y apoyo incondicional en los momentos más desafiantes. A "Los Cocos", gracias por ayudarme a redescubrir la alegría en la vida.

Finalmente, mi sincero agradecimiento a la Universidad Yachay Tech, por brindarme una educación de calidad y por ser un espacio de crecimiento académico y personal.

A todos, les estoy profundamente agradecido. Este logro es también suyo.

Daniel Alexander Pijal Morejón

Resumen

La investigación geológica en las costas de Ecuador ha despertado un creciente interés debido a su intrincada historia geológica y estratigráfica, especialmente notoria en la Cuenca Borbón-Esmeraldas, localizada en el norte del país. Este territorio se caracteriza por una rica estratigrafía secuencial proveniente de una cuenca de antepaís, proporcionando una perspectiva excepcional sobre los procesos deposicionales y tectónicos que han formado la cuenca a lo largo de millones de años. Comprender estas secuencias estratigráficas es esencial para el progreso en el campo geológico y para descifrar la dinámica de los cambios ambientales.

El análisis se lleva a cabo mediante una metodología integrada que incluye análisis sísmicos y registros de perforación, complementados con técnicas geofísicas de última generación como Noise2Void y Spectral Blueing. Esta estrategia enriquece la calidad de las imágenes del subsuelo y facilita interpretaciones geológicas detalladas de la estratigrafía secuencial, promoviendo un estudio más exhaustivo de las complejas secuencias estratigráficas de la región.

Los descubrimientos indican la transformación geológica de la cuenca de Borbón-Esmeraldas desde el Cretácico Tardío hasta el Pleistoceno, subrayando una notable mejora en la calidad de los datos sísmicos gracias a las técnicas avanzadas que simplifican la interpretación geológica. Se han identificado cinco secuencias estratigráficas, junto con 5 disconformidades, cada una relacionada a una fase tectónica las cuales se han correlacionado con variaciones en el nivel del mar y con formaciones geológicas concretas, evidenciando una compleja relación entre la deposición sedimentaria, la actividad tectónica y la erosión. Este análisis ofrece una visión completa de los cambios ambientales y deposicionales.

Palabras Clave:

Estratigrafía secuencial, mejoramiento de datos sísmicos, registros de pozo.

Abstract

Geological exploration on the Ecuadorian coasts has generated increasing interest due to its complex geological and stratigraphic history, particularly in the Borbón Esmeraldas Basin, located in northern Ecuador. This region stands out for its rich sequential stratigraphy formed by a back-arc, offering a unique window into the depositional and tectonic processes that have shaped the basin over millions of years. Understanding these stratigraphic sequences is fundamental to advancing our geological knowledge and elucidating the dynamics of environmental changes.

The study adopts an integrated methodology, using seismic analysis and well logs, complemented by advanced geophysical techniques such as Noise2Void and Spectral Blueing. This approach improves the quality of subsurface images and facilitates precise geological interpretations of the sequential stratigraphy, allowing for a deeper investigation of the region's complex stratigraphic sequences.

The discoveries indicate the geological transformation of the Borbón-Esmeraldas basin from the Late Cretaceous to the Pleistocene, highlighting a notable improvement in the quality of seismic data thanks to advanced techniques that simplify geological interpretation. Five stratigraphic sequences have been identified, along with 5 unconformities, each related to a tectonic phase. These have been correlated with variations in sea level and with specific geological formations, showing a complex relationship between sedimentary deposition, tectonic activity, and erosion. This analysis provides a comprehensive view of the environmental and depositional changes.

Keywords:

Sequential stratigraphy, seismic data improvement, well-logs.

Contents

Dedication	iii
Acknowledgment	iv
Resumen	v
Abstract	vi
Contents	vii
List of Tables	x
List of Figures	xi
1 Introduction	1
1.1 Study Area	2
1.2 Background	3
1.3 Objectives	5
1.3.1 General Objective	5
1.3.2 Specific Objectives	5
1.4 Justification	6
1.5 Methodology	7
1.6 Introduction to Sequence Stratigraphy	8
1.6.1 Principles of Sequence Stratigraphy	8
1.6.2 Discontinuities	9
1.7 Processing Techniques to Improve the Quality of Seismic Data	11
1.8 Subsidence	11

2	Geological Framework	13
2.1	South America	13
2.2	Main geological features of the Ecuadorian Coast	14
2.3	The Esmeraldas-Borbón Basin	16
3	Database and Methodology	19
3.1	Database	19
3.1.1	Seismic lines	20
3.1.2	Well log	21
3.2	Methodology	22
3.2.1	Quality Control	23
3.2.2	Generation of Pseudo-Sonic Logs	25
3.2.3	Seismic Well Tie	27
3.2.4	Seismic Data Improvement	28
3.2.5	Second Synthetic Seismogram and Seismic Well Tie	31
3.3	Seismic Interpretation	31
3.3.1	Depositional Sequences and Sedimentary Framework	32
3.3.2	Isopach Maps	33
3.3.3	Geohistorical graphics	34
4	Stratigraphy of the Borbón Esmeraldas Basin	36
4.1	Lithostratigraphy	37
4.1.1	Piñón Formation	39
4.1.2	Santiago Formation	39
4.1.3	Zapallo Formation	40
4.1.4	Pambil Formation	40
4.1.5	Viche Formation	40
4.1.6	Angostura Formation	40
4.1.7	Onzole Formation	41
4.1.8	Borbón Formation or Cachabí Formation	42
4.1.9	Alluvial Deposits and Terraces	42
4.2	Biostratigraphy	43

4.3	Paleoenvironment	45
5	Results	47
5.1	Seismic data improvement	47
5.2	Sequence stratigraphy	49
5.2.1	Major unconformities	50
5.2.2	Basement	52
5.2.3	Sequence stratigraphy A (Middle to Late Eocene)	54
5.2.4	Sequence stratigraphy B (Middle Oligocene to Late Oligocene)	56
5.2.5	Sequence stratigraphy C (Early Miocene to Middle Miocene)	56
5.2.6	Sequence stratigraphy D (Late Miocene)	58
5.2.7	Sequence stratigraphy E (Oligocene to Pleistocene)	59
5.3	Subsidence analysis	61
5.3.1	Borbón-1	62
5.3.2	Telembí-1	63
6	Discussion	66
6.1	Sedimentation and Tectonic history of the Esmeraldas Borbón Basin	66
6.1.1	First tectonic phase: Latest Cretaceous–Paleocene	66
6.1.2	Second tectonic phase: Late Eocene–Early Oligocene	67
6.1.3	Third tectonic phase: Late Oligocene–Early Miocene	67
6.1.4	Fourth tectonic phase: Middle Miocene	67
6.1.5	Fifth tectonic phase: Early Pliocene to Present	68
7	Conclusions	69
	Bibliography	71
	Appendices	75
.1	Appendix 1.	78

List of Tables

3.1	Seismic Line Catalog: this table provides a detailed inventory of the seismic lines analyzed within the area of this study, the location of the seismic lines is shown in Figure 1.1.	20
3.2	Well-Log Data of Borbón-1 and Telembí-1: This table compiles data from two wells, including measurements of Natural Gamma Ray (LN), Spontaneous Potential (SP), Sonic Neutron (SN), P-wave velocity (Vp), and Resistivity (RES), and N/A is Not Applicable. Each column represents a distinct well log used to characterize subsurface geological formations. The location of the well-logs is shown in Figure 1.1	21

List of Figures

1.1	Study Area: This map offers an accurate illustration of the study area, encapsulated within a blue rectangle with the geology of the Esmeraldas province in the background. Solid black lines cross the area, representing the seismic lines integral to the investigation, while red dots denote the wells. Based on Reyes and Michaud (2012)	2
2.1	Map of the Location of Major Basins along the Ecuadorian Coast: This comprehensive map vividly delineates the major fault lines across the region and pinpoint the locations of the Esmeraldas-Borbón Basin, the Manabí Basin, and the Progreso Basin, along with Ecuador’s principal geological structures. Modified from Tamay Granda et al. (2018) ; Jaillard et al. (1997)	15
2.2	Geologic map of the Esmeraldas-Borbón Basin: This detailed representation showcases the geological outcrops of the main formations, as well as the basin’s major geological faults and structures. Based on Reyes and Michaud (2012)	17
3.1	Schematic Overview of the Research Methodology: This figure provides a schematic representation of the research methodology, detailing the sequential steps and processes from the study’s inception through to its conclusion.	23

3.2 Linearization of $Z \times R$ vs. V_P for determining constants a and m : This figure presents the linear relationship between the product of impedance (Z) and resistivity (R) plotted against P-wave velocity (V_P), utilized to identify the constants a and m . The graph demonstrates the method for extracting these constants, crucial for quantifying the geological and petrophysical parameters of the subsurface formations. 26

3.3 Comparison of Real VP Records (Blue) with Pseudo-Sonic Log (Orange): This figure illustrates a side-by-side comparison of actual P-wave velocity (VP) records, depicted in blue, against the pseudo-sonic log data, shown in orange. It visually contrasts the measured VP values from well logs with those derived from the pseudo-sonic methodology, highlighting the accuracy and discrepancies between these two approaches in evaluating subsurface velocities. 27

3.4 Schematic Illustration of the Noise2Void Denoising Procedure: This diagram depicts the step-by-step process of the Noise2Void technique for removing noise from images without the need for clean training data. By intelligently sampling pixels and predicting their values based solely on the surrounding pixel information, the algorithm effectively reduces noise while preserving the integrity of the original image content (Birnie et al., 2021). 30

3.5 Second Synthetic Seismogram with Wavelet Post-Seismic Data Improvement and Final Well-Seismic Tie. This figure depicts the second iteration of a synthetic seismogram, incorporating an optimized wavelet based on refined seismic data. Including the correlation coefficient ($r = 0.99$) that improved compared to the first synthetic seismogram. 32

3.6 Seismic Line 3A: *Color-Coded Horizon Interpretation* - Horizons are distinctly marked for clarity: Piñón in purple, Zapallo in red, Pambil in yellow, Viche in blue, and Angostura in green. Interpreted faults are delineated in black, providing a comprehensive visual guide to the geological structure. 33

3.7 Geohistorical Graph Illustrating Subsidence: This graph represents total subsidence, denoted as H , with specified time intervals (T_0 - T_n) and Z representing depth. 35

4.1	Outline of the distinct areas within the Esmeraldas Borbón Basin including: a) the West Zone (WZ), b) the Elevated Central Zone (CZ), and c) Northeast Zone (NZ). Based on the map of Ordoñez et al. (2006)	36
4.2	Generalized Stratigraphic Column of the Esmeraldas-Borbón Basin: Show principal geological formations and key hiatuses. Based on Jaillard et al. (1997) ; Deniaud (2000) ; Marcaillou and Collot (2008) ; Reyes and Michaud (2012)	38
5.1	Comparison of a zoom in to the Seismic Line 1A data before and after denoising: a) Original seismic line 1A image before the denoising process, highlighting the presence of noise. b) The same seismic line 1A following the application of denoising techniques, with a circle emphasizing a sig- nificant improvement in data clarity , demonstrating the effectiveness of the denoising process in removing unwanted noise.	48
5.2	Effects of Spectral Blueing on of a zoom in to the Seismic Line 10B: The images display seismic lines before (in the row 1) and after (in the row 2) the application of Spectral Blueing. In images a) and c), Spectral Blueing ac- centuates specific frequencies, aiming to enhance seismic resolution. While, image b) demonstrates enhanced continuity of seismic lines, making a fault (marked with a yellow line) more visibly distinct.	49
5.3	Seismic line 3A: showing the representative reflectors within each sequence (A to E) to illustrate their geometry, along with the unconformities Ub, U1, U2, U3, U4. To see the location of the seismic line consult the Figure 1.1. .	50
5.4	Correlation between seismic units A to E of the Esmeraldas Borbón Basin and the unconformities Ub to U4 in relation to the geological formations. This visualization includes a detailed focus on seismic line 3A, highlight- ing the key features and the interaction between the seismic units and the geological formations. The Esmeraldas Borbón basins is based on: Pre- Oligocene chronostratigraphy is from (Jaillard et al., 1997); the Neogene chronostratigraphy is from (Deniaud, 2000 ; Marcaillou and Collot, 2008 ; Reyes and Michaud, 2012)	51

5.5 Schematic Sequential Stratigraphy of the Borbón-Esmeraldas Basin: This illustration encapsulates comprehensive log data from Borbón-1, including Lithium Neutron (LN) logs in porosity (percentage), Sonic Neutron (SN) logs in microseconds per foot (us/ft), Spontaneous Potential (SP) in millivolts (mV), and P-wave Velocity (Vp) in feet per second (ft/s). The figure meticulously outlines the corresponding lithologies for each formation, sequences from A to E, identifies unconformities and boundaries with second-order, transgressive-regressive (T-R) cycles, paleobathymetry, and integrates the Eustatic curve following [Haq et al., 1987], providing a detailed view of the basin’s stratigraphic dynamics. 53

5.6 a) Seismic Line A3 (location in Figure 1.1); b) a segment of Seismic Line A3 selected for constructing stratigraphic sequences, highlighting representative reflectors within each sequence to illustrate their geometry—the (location of this segment is marked by a yellow box); c), d), e), and f) present detailed views of the seismic profile from Seismic Line 3A (detailed section is identified by orange boxes). 54

5.7 Isopach Map of Sequence Stratigraphy A (Middle to Late Eocene): This map showcases the distribution of sediment thickness across the region, where sediment accumulation is maximized (depocenter), are clearly delineated alongside structural highs. 55

5.8 Isopach Map of Sequence stratigraphy B (Middle Oligocene to Late Oligocene): This map showcases the distribution of sediment thickness across the region, where sediment accumulation is maximized (depocenter), are clearly delineated alongside structural highs. 57

5.9 Sequence stratigraphy C (Early Miocene to Middle Miocene): This map showcases the distribution of sediment thickness across the region, where sediment accumulation is maximized (depocenter), are clearly delineated alongside structural highs. 58

5.10 Sequence stratigraphy D (Late Miocene): This map showcases the distribution of sediment thickness across the region, where sediment accumulation is maximized (depocenter), are clearly delineated alongside structural highs. 60

5.11	Geohistorical Chart of Borbón-1 Well: This chart provides a detailed view of the chronological development and sedimentary sequences within the Borbón-1 well, illustrating Sequences A, B, C, D, and E. It also marks the key unconformities U1, U2, U3, and U4.	63
5.12	Geohistorical Chart of Telembí-1 Well: This chart provides a detailed view of the chronological development and sedimentary sequences within the Borbón-1 well, illustrating Sequences A, B, D, and E. It also marks the key unconformities U1, U2, and U4.	65
1	a) Seismic Line A2 (location in Figure 1.1); b) a segment of Seismic Line A3 selected for constructing stratigraphic sequences, highlighting representative reflectors within each sequence to illustrate their geometry—the (location of this segment is marked by a yellow box); c), and d) present detailed views of the seismic profile from Seismic Line 3A (detailed section is identified by orange boxes).	78

Chapter 1

Introduction

The northern sector of the Ecuadorian coastal basins has been the focus of geological research for several decades, mainly due to its unique position along the Pacific margin and its complex tectonic and depositional history. Previous studies in this area have laid the groundwork, identifying key stratigraphic units, outlining the overall structural configuration, and hypothesizing the geological processes at play. However, these investigations were often based on limited data sets and conventional analysis techniques, offering a fragmented understanding of the region's geological framework. This backdrop of preliminary explorations and growing scientific curiosity sets the stage for the current study, which aims to leverage newer, more sophisticated analytical methods to provide a complete and refined view of the basin's stratigraphic sequence.

The exploration of the sequence stratigraphy within the northern part of the Ecuadorian Coastal Basins, through the synergistic use of seismic and well-log data, marks a pivotal effort in unraveling the complex depositional history and the spatiotemporal evolution of this region. This study aims to meticulously reconstruct the stratigraphic sequences of the northern Ecuadorian coast basin, thereby enriching our understanding of its geological past and providing a detailed account of its development over time.

This Undergraduate Thesis unfolds across seven chapters, designed to progressively articulate and analyze the subject matter. The introductory Chapter 1 sets the stage by outlining the thesis theme, incorporating a literature review, objectives, a succinct methodology overview, and an introduction to the core theoretical concepts. Chapter 2 deepens into the regional geological context and the distinctive geological characteristics of

the northern Ecuadorian coastal basins, establishing a solid foundation for understanding the area's geological complexity. Chapter 3 provides an exhaustive presentation of the data and methodologies employed, emphasizing the rigorous approach taken in data analysis and interpretation. Chapter 4 shows the stratigraphic fill of the basin, biostratigraphy, and facies. Chapter 5 is dedicated to the exposition of results, focusing on the elucidation of key stratigraphic sequences, hiatuses, discontinuities, and contacts discovered during the study. Chapter 6 shows the discussion on the formation history of the basin. Conclusively, Chapter 7 synthesizes the main conclusions, reflecting on the study's findings and their implications.

1.1 Study Area

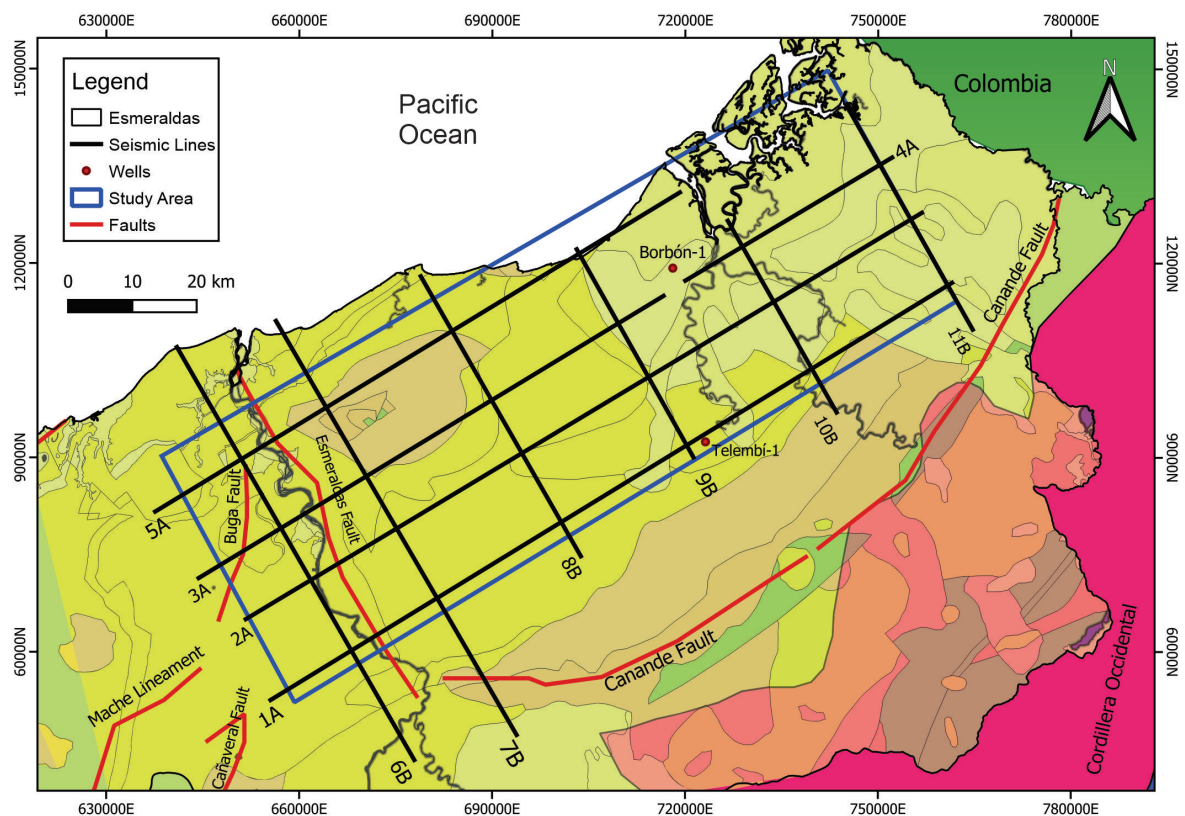


Figure 1.1: Study Area: This map offers an accurate illustration of the study area, encapsulated within a blue rectangle with the geology of the Esmeraldas province in the background. Solid black lines cross the area, representing the seismic lines integral to the investigation, while red dots denote the wells. Based on [Reyes and Michaud \(2012\)](#).

The thesis centers on the study of basins located in the northern part of the Ecuadorian coast, primarily focusing on the Esmeraldas and Borbón basins. This research considers these basins collectively as a single entity, known as the Borbón-Esmeraldas basin. This unified approach allows for an integrated examination of the area, which is distinguished by its geographical boundaries. Acting as the northern limit between Ecuador and Colombia, the region extends from the Mataje River in the north to the Canande fault in the south and is flanked by the foothills of the Western Cordillera to the east and the Pacific Ocean to the west. The strategic positioning of the Borbón-Esmeraldas basin, covering a significant expanse of the Ecuadorian-Colombian border from the foothills of the Western Cordillera to the Pacific Ocean, emphasizes its relevance for geological investigations and sequence stratigraphic analyses.

The designated study polygon, outlined by seismic lines and wells, captures a substantial area of the combined Esmeraldas and Borbón basins within the Borbón-Esmeraldas basin complex, as depicted in Figure 1.1. This delineation secures a broad area for in-depth geological exploration, enabling thorough interpretations that underpin the examination of this crucial region's geological characteristics and sequence stratigraphy.

1.2 Background

Variable interactions between converging tectonic plates form forearc basins. The regions affected during convergence are subjected to shortening, extension, and strike-slip deformation modes, generating different formations such as folds, reverse and normal faults, and geological structures (Horton, 2018). Structurally, the forearc region includes forearc basins, an outer arc, an accretionary prism, and the trench itself. The sedimentary basin lies between the separation and the magmatic arc and is filled primarily with erosive matter from the volcanic arc (Kearey et al., 2009).

The forearc of the northern part of the Ecuadorian coast is related to the convergence of the Caribbean Plate and the South American Plate during the Upper Cretaceous (Aizprua et al., 2019). However, the Caribbean plate is juxtaposed with the North American, Cocos, and Nazca plates via subduction and transform plate boundary zones (Luzieux, 2007). For the forearc of the Ecuadorian coast, the most critical process was that the margin

of northern South America was deformed synchronously with the fragmentation of the Caribbean Plate ([Luzieux, 2007](#)) and was not consumed by subduction due to its buoyancy ([Closs, 1993](#)). Evidence for these interactions is found in mafic sequences with oceanic plateau affinities that are documented in the Western Cordillera, the coastal flat forearc region, and the high seas regions of Ecuador and Colombia ([Kerr et al., 2002](#)), which are partly believed to have broken away from the Caribbean Plateau ([Spikings et al., 2001a](#)). Furthermore, evidence of these interactions has also been found along the forearc basins from northern Peru to the Caribbean coast ([Nygren, 1950](#)). Consequently, the basins of the Ecuadorian coast, such as the Esmeraldas-Borbón basin, Manabí Basin, and Progreso Basin, are also linked to the basins of western Colombia, primarily with Tumaco Basin. In Ecuador, this part of the forearc is also related to a process of subduction of Carnegie Ridge ([Daly, 1989](#); [Benitez, 1995](#)), which affects the Progreso, Manabí, and Esmeraldas-Borbón basins.

While the chronostratigraphic interpretations and geological structures of the Tumaco and Borbón basins have been elucidated through a combination of field geology, seismic reflection profiles, and well drilling data ([Evans and Whittaker, 1982](#)), the sequence stratigraphy interpretations across the basins in the northern part of the Ecuadorian coast are either not well understood or considered to be of inferior quality ([Marcaillou and Collot, 2008](#)). There is a significant knowledge gap in understanding the behavior and evolution of the geologically complex northern part of the Ecuadorian Coastal Basins. Previous studies on sequence stratigraphy such as [Evans and Whittaker \(1982\)](#); [Marcaillou and Collot \(2008\)](#); [Luzieux \(2007\)](#) have left this area incomplete. To comprehensively address this gap, it is essential to delve into the sequence stratigraphy by integrating seismic and well-log data. This research aims to decipher the development and spatial-temporal distribution of depositional systems.

From an economic perspective, the basins that are related to subduction processes are not linked to hydrocarbon reserves; Even so, the Bourbon sub-basin, due to the thickness of the sediments and the deepening offshore, is a prospective area for the exploration of hydrocarbons. The International Ecuadorian Petroleum Company (IEPC) drilled the Borbón-1 well very close to Borbón within the Santiago River Basin, where trace samples of hydrocarbons were found ([Galvez and Gutierrez, 2005](#)). Although the Esmeraldas sub-

basin volcanic rock basement is found at a shallow depth, it is not prospective. The Camarones-1 well drilled by the IEPC is proof of that. Also, there is a history of productive oil fields in forearc basins worldwide (Hessler and Harman, 2018). As a result, it is essential to understand and interpret basin evolutionary processes by sequential stratigraphy.

From an economic perspective, the discovery of trace samples of hydrocarbons in the Borbón-1 well drilled by the International Ecuadorean Petroleum Company underscores the potential significance of the region. This finding, as reported by Galvez and Gutierrez (2005), highlights the need for a more detailed and systematic investigation into the sequence stratigraphy to understand the reservoir potential better and facilitate informed decision-making in the oil and gas industry.

Moreover, the historical success of productive oil fields in forearc basins worldwide, as demonstrated by Hessler and Harman (2018), further emphasizes the importance of the northern Ecuadorean Coastal Basins as a prospective area for hydrocarbon exploration. However, to leverage this potential, a comprehensive sequence stratigraphic analysis is imperative for identifying favorable depositional environments and enhancing the accuracy of reservoir characterization.

Therefore, this research addresses the limitations of previous studies and aligns with the region's economic interests. It provides a more detailed understanding of the sequence stratigraphy, contributing to exploring and exploiting hydrocarbons in the northern Ecuadorean Coastal Basins.

1.3 Objectives

1.3.1 General Objective

Reconstruct the northern Ecuadorean coast basin's sequence stratigraphy to enhance understanding of its depositional history and spatiotemporal evolution

1.3.2 Specific Objectives

- Improve seismic and well-log data quality and resolution using advanced techniques.
- Conduct a rigorous well-tie analysis for accurate correlation between well logs and

seismic data and perform detailed seismic interpretation to elucidate key geological features.

- Merge petrophysical, seismic, and well data analyses into a unified sequence stratigraphy model to capture the area's geological complexity. Develop a comprehensive framework that integrates diverse data for a detailed understanding of the geology of the northern Ecuadorian coast.
- Develop a detailed chronological framework of the tectonic events in the Borbón Esmeraldas basin, utilizing geophysical.

1.4 Justification

The justification for this thesis on the sequence stratigraphy of the northern part of the Ecuadorian Coastal Basins rests on several compelling arguments. Primarily, the current body of research, referenced by studies such as [Marcaillou and Collot \(2008\)](#); [Aizprua et al. \(2019\)](#); [Evans and Whittaker \(1982\)](#), falls short of providing a comprehensive understanding of the area's main basins, notably the Borbón-Esmeraldas basin. This shortfall creates a significant knowledge gap, obstructing precise geological interpretations and restricting the effective application of findings in resource exploration and exploitation. Additionally, the economic potential highlighted by the discovery of hydrocarbon traces in the Borbón-1 well calls for an in-depth analysis of sequence stratigraphy to pinpoint promising depositional environments and improve reservoir characterization. The documented success of forearc basins globally, including in studies such as [Hessler and Harman \(2018\)](#), further indicates the potential of the northern Ecuadorian Coastal Basins for hydrocarbon exploration, underscoring the necessity of detailed sequence stratigraphic study for informed decision-making and risk mitigation.

The advent of recent technological advancements in seismic and well-log data acquisition and processing offers an unprecedented opportunity to refine the quality and resolution of geological interpretations. Utilizing these advancements is crucial for achieving a more precise and comprehensive reconstruction of the area's sequence stratigraphy. This research's enhanced understanding of depositional history and spatiotemporal evolution not only aids

in efficient resource management but also promotes the sustainable utilization of natural resources, mitigating environmental impacts and catering to escalating energy needs. From a scientific perspective, this thesis aims to bridge the existing gaps in sequence stratigraphy within the northern Ecuadorian Coastal Basins, laying the groundwork for subsequent research and enriching the geological science discipline. The industry relevance of this study cannot be overstated, as accurate sequence stratigraphic models are essential for minimizing exploration risks, optimizing drilling locations, and enhancing reservoir management tactics in the oil and gas industry. In essence, this thesis is poised to fill critical knowledge gaps, align with economic imperatives, harness technological innovations, contribute to global geological insights, advocate for sustainable resource use, and significantly influence industry practices.

1.5 Methodology

The methodology adopted for this research is thoughtfully structured into two pivotal stages: geophysical analysis and geological interpretation. Each stage plays a crucial role in piecing together a holistic understanding of the study area's geological framework. A brief explanation of the methodology used for this thesis will be given below, but it will be better detailed in Chapter 3.

Geophysical Analysis Stage: The onset of the study is marked by a detailed geophysical examination of the seismic reflection data. This stage is foundational, focusing on the calibration of seismic data with well log information to accurately identify and correlate geological features across the seismic profiles. It involves rigorous processing and analysis of seismic data to refine the resolution and clarity of seismic reflections, thereby enabling precise identification of stratigraphic horizons, faults, and other subsurface structures.

This thesis capitalizes on seismic reflection data provided by the Ministerio de Energía y Minas (Government of the Republic of Ecuador). The core of the subsurface data compilation encompasses eleven 2D seismic reflection lines, which are synergistically integrated with data from two wells. This integration facilitates the creation of a seismic-well tie, significantly enhancing the quality of the seismic profiles and thereby, the reliability of the interpretations derived from them.

Geological Interpretation Stage: Following the geophysical analysis, the geological interpretation stage seeks to contextualize the seismic data within the broader geological setting of the area. This involves interpreting the refined seismic profiles to delineate depositional environments, sequence stratigraphy, and the geological history of the region. The integration of seismic data with well logs and other geological information allows for a comprehensive interpretation of the subsurface geology, revealing insights into the temporal and spatial evolution of the study area's sedimentary sequences.

Together, these stages encompass a methodological approach that leverages high-quality seismic and well data, combining technical rigor with geological insight to unravel the complex geological dynamics of the study area.

1.6 Introduction to Sequence Stratigraphy

Sequence stratigraphy is an integrative approach that examines sedimentary deposits through the prism of depositional sequences and systems tracts, encapsulating variations in sea level, sediment supply, and accommodation space (Catuneanu and Eriksson, 2007). This method extends beyond conventional sedimentary basin analysis, offering insights into the temporal and spatial distribution of depositional environments.

Unlike litho-stratigraphy, sequence stratigraphy evaluates the stratigraphic record within a time-stratigraphic framework, employing unconformities that signify temporal discontinuities in the geological record. These key surfaces facilitate the identification of sequences associated with shifts in relative sea level, enabling their correlation across regional to intercontinental scales. This broader perspective aids in interpreting stratigraphic architecture and predicting sedimentary facies, enhancing our understanding of sedimentary basin dynamics.

1.6.1 Principles of Sequence Stratigraphy

The principles of sequence stratigraphy are fundamental in deciphering the depositional patterns and stratigraphic architectures of sedimentary basins. This discipline interprets sequences of rock layers in relation to fluctuating sea levels, sediment supply, and subsidence rates, establishing a framework that connects sedimentary deposits with temporal

scales and environmental transformations (Catuneanu and Eriksson, 2007). In the Northern Ecuadorian Coastal Basins, these principles are instrumental in correlating seismic and well-log data, enabling a detailed reconstruction of the basin's geological history. Identifying sequence boundaries, systems tracts, and parasequences is critical for stratigraphic mapping and understanding the evolution of depositional environments over geological time.

Sequence stratigraphy delves into rock relationships within a chronostratigraphic framework, emphasizing the concept of accommodation space (the total space available for potential sediment accumulation). Accommodation arises from relative sea-level changes, influenced by eustatic changes, tectonic subsidence, and sedimentation rates. Within the Ecuadorian Coastal Basins, the interplay among these factors is encapsulated in the stratigraphic sequences. By analyzing these sequences through seismic and well-log data, researchers can glean insights into historical climatic conditions, tectonic activities, and sedimentary processes. Consequently, the sequence stratigraphic methodology is invaluable for predicting the distribution of reservoir and non-reservoir facies, playing a pivotal role in the hydrocarbon exploration and exploitation efforts in the region.

1.6.2 Discontinuities

Discontinuities in stratigraphic sequences represent critical interruptions in sedimentary deposits that reflect changes in depositional environments, erosion, or other geological processes. These discontinuities can range from global unconformities to local erosional surfaces and are essential for understanding the geological history of an area. Also, unconformities and sequence boundaries play a crucial role in sequence stratigraphy, delineating changes in sedimentary conditions often related to sea-level fluctuations, tectonics, and sediment supply.

Sequence boundaries represent the lower limits of sequences, which are packages of genetically related strata. They are critical for understanding the architecture of sedimentary records and for reconstructing past environmental changes, including sea level fluctuations, tectonic movements, and sediment supply variations.

Sequence boundaries arise from various processes that interrupt sediment deposition and can include subaerial exposure, erosion, or non-deposition. These processes are typ-

ically driven by relative changes in sea level, tectonic uplift, or a significant reduction in sediment supply. The formation of a sequence boundary is generally associated with a fall in relative sea level, leading to erosion or non-deposition on a regional scale. This fall in sea level exposes the continental shelf and can lead to the development of an erosional unconformity, or a sequence boundary, which is a time-significant break in the sedimentary record.

Two main types of sequence boundaries are recognized:

- **Type 1 Sequence Boundary:** This occurs when there is a significant fall in sea level, leading to subaerial exposure and erosion of continental margins. The erosion can result in a pronounced unconformity that can be traced across large areas. Type 1 sequence boundaries are typically associated with lowstand systems tracts, where sedimentation occurs mainly in deep-water settings due to the significant drop in sea level.
- **Type 2 Sequence Boundary:** This type is associated with a less pronounced fall in sea level or its rise, where the rate of sedimentation keeps pace with or exceeds the rate of sea-level change. Type 2 sequence boundaries may not exhibit significant erosional features but are characterized by a change in sedimentation patterns. They are often marked by a conformity or a slight disconformity in marine settings and are associated with highstand and transgressive systems tracts.

Unconformities are fundamental stratigraphic surfaces that indicate a discordant relationship between strata. They play a key role in sequence stratigraphy by marking the boundaries between sequences, which are packages of genetically related strata. The study of unconformities helps to unravel complex geological meanings and aids in the understanding of tectonic cycles, sedimentary processes, and the chronostratigraphic significance of sequences ([Ming-xiang, 2011](#)).

Unconformities can be generated by various processes, including tectonic uplift, sea-level changes, and erosional events. They are characterized by missing time in the geological record and can be divided into several types based on their formation mechanisms, such as angular unconformities, disconformities, and paraconformities. The study and

classification of unconformities are crucial for constructing accurate sequence stratigraphic frameworks and for interpreting the sedimentary history of basins (Weimer, 1993).

1.7 Processing Techniques to Improve the Quality of Seismic Data

Enhancing the quality of seismic data is paramount for accurate geological interpretation. This thesis introduces a pioneering two-step methodology designed to augment seismic data quality, thereby refining its utility for geological analysis. The initial phase of this methodology employs Denoising with Noise2Void (N2V), an advanced neural network technique that effectively reduces noise without the necessity for clean training data. This approach leverages the inherent patterns within noisy datasets to identify and mitigate unwanted noise, setting a robust foundation for subsequent processing steps.

Following the denoising phase, the methodology incorporates Spectral Blueing, a technique specifically aimed at enhancing higher frequencies within the seismic data. This step is crucial for achieving a balanced spectral distribution, which is instrumental for improving both resolution and interpretability of the seismic information. Spectral Blueing adjusts the amplitude spectrum to emphasize higher frequencies, compensating for the natural attenuation of these components during seismic wave propagation.

The synergy of Denoising with Noise2Void and Spectral Blueing represents a significant leap forward in seismic data processing techniques. By addressing both noise reduction and frequency balance, this two-step approach offers the potential to greatly enhance the clarity and resolution of seismic datasets, facilitating more precise geological interpretations and advancing the field of seismic data analysis for geological studies.

1.8 Subsidence

According to Steckler and Watts (1978) subsidence refers to the gradual sinking or settling of the Earth's surface. It is a natural process that can result from a variety of factors including the compaction of sediment, tectonic activities, and the extraction of underground resources. Understanding subsidence is crucial for interpreting sedimentary basin

development and the Earth's geological history.

In geology, the visualization of subsidence over time is critical. A Geohistorical Graph or Subsidence-Time Graph represents the relationship between subsidence and time, providing a summary of historical subsidence rates and aiding in the analysis of geological processes.

The total subsidence, denoted as H , is calculated over predetermined time intervals, capturing significant epochs or stages in the geological timeline. This value is crucial for constructing accurate geohistorical graphs that track the subsidence of the Earth's surface over time. These calculations are based mainly on ([Allen and Allen, 2013](#)).

Chapter 2

Geological Framework

2.1 South America

The geology of South America is a testament to the continent's dynamic and complex Earth history, characterized by the interaction of plate tectonics, volcanic activity, and sedimentary processes over billions of years. This interaction involves the movement and collision of several major and minor tectonic plates, including the South American Plate, the Nazca Plate, the Caribbean Plate playing a pivotal role in shaping the continent's geological landscape. This rich geological tapestry has given rise to diverse landscapes, from the majestic Andes mountains to the extensive Amazon basin and the ancient cratons of the Guiana Shield. Within this broader geological framework, the coastal basins from Perú to Panamá stand out due to their unique tectonic settings, sedimentation histories, and the influence of oceanic processes.

The Northern Andean convergent margin features extensive Cenozoic forearc basins stretching from northern Peru to Panama, with notable basins in Western Colombia and along the Ecuadorian coast ([Bueno Salazar, 1989](#); [Jaillard et al., 1997](#)). Key basins in Western Colombia include the Uraba, Atrato-San Juan, and Tumaco Basins, while the Borbón, Manabí, and Progreso Basins are prominent along the Ecuadorian coast, to view the map of the major river basins in South America, please consult the Figure in [Marcaillou and Collot \(2008\)](#). This arrangement highlights the region's geological complexity and its significance in understanding tectonic and sedimentary evolution.

The Cenozoic forearc basins along the Northern Andean convergent margin, stretching

from northern Perú to Panamá, shaped by the accretion of the Caribbean Large Igneous Province (CLIP) to the South American margin since the Late Cretaceous and the early Cenozoic post-collisional convergence between the Farallon and South American plates. This process facilitated the development of a series of basins across the Northern Andean margin. The formation of these basins is associated with tectonic activity related to subduction, where the movement and interaction of tectonic plates played a crucial role in their evolution. The basins developed on isolated basements formed by accreted blocks of oceanic or transitional crust, trapped between the arc massif and the subduction zone, reflecting a complex history of sedimentation and tectonic deformation over time.

This study zeroes in on the crucial basins along the northern Ecuadorian coast, with particular focus on the Borbón Esmeraldas basin. Situated along the Pacific coast of Ecuador, the Borbón-Esmeraldas basin is strategically positioned between significant geological landmarks that both delineate its boundaries and shape its unique geological framework. Stretching from the Mataje to the Canande fault, and flanked to the east by the Western Cordillera's foothills and to the west by the Pacific Ocean, this basin not only straddles a notable portion of the Ecuadorian-Colombian border but also underscores its significance in geological investigations and sequence stratigraphy. Characterized by intricate stratigraphy shaped by the interplay of tectonic forces from the subduction of the Nazca Plate beneath the South American Plate, the basin hosts a variety of depositional environments and sedimentary processes. This complex geological setup renders the Borbón-Esmeraldas basin a key site for delving into the sedimentary dynamics and evolutionary trajectory of Ecuador's coastal territories and the expansive Andean margin.

2.2 Main geological features of the Ecuadorian Coast

The coastal geology of Ecuador is characterized by several key basins, specifically the Esmeraldas-Borbón Basin located in the northern part of the Ecuadorian coast, the Manabí Basin to the south, and the Progreso Basin near the Gulf of Guayaquil, as illustrated in Figure 2.1. These will be described in detail below. The geological setting of Ecuador's coast stands as a testament to dynamic Earth processes, including subduction and plate tectonics, sedimentary basin formation, and volcanic activity.

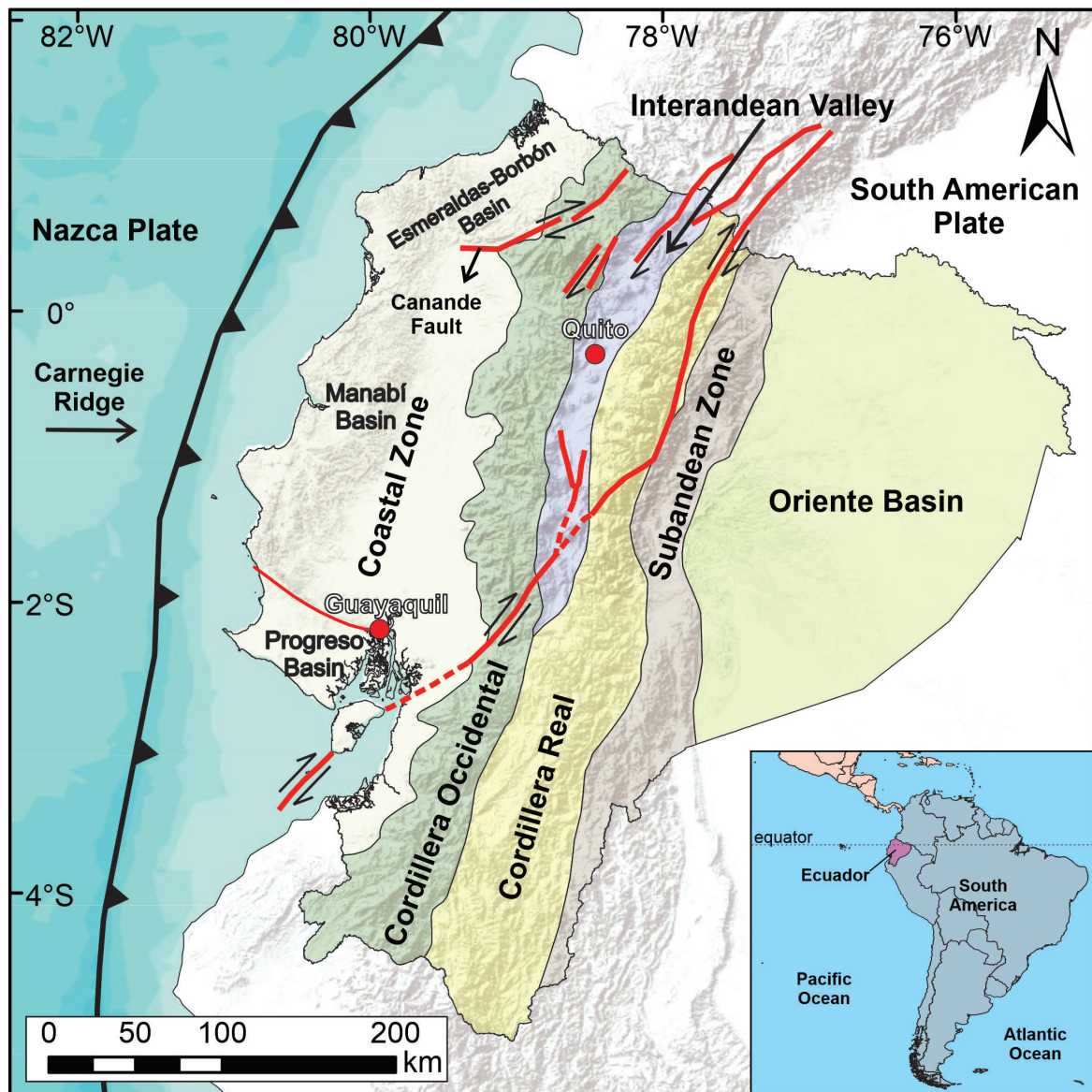


Figure 2.1: Map of the Location of Major Basins along the Ecuadorian Coast: This comprehensive map vividly delineates the major fault lines across the region and pinpoint the locations of the Esmeraldas-Borbón Basin, the Manabí Basin, and the Progreso Basin, along with Ecuador's principal geological structures. Modified from [Tamay Granda et al. \(2018\)](#); [Jaillard et al. \(1997\)](#)

- **Esmeraldas-Borbón Basin**

This basin, located in northwest Ecuador, as illustrated in the Figure 2.1, comprises a sequence predominantly of Tertiary mudstones interspersed with shallow-water sandstones, underlain by a Cretaceous basaltic basement. The stratigraphic record begins with middle Eocene thin, discontinuous turbiditic carbonates, evolving into a

thick sequence of mudstones extending into the mid-Miocene. Late Miocene to early Pliocene saw the deposition of shallow-water sandstones, followed by deeper water mudstones in the Pliocene. The area has been subject to NE-SW-trending folding, parallel to the mid-slope basement high, suggesting significant post-late Pliocene tectonic activity (Evans and Whittaker, 1982).

- **Manabí Basin**

Manabí Basin is along the central Ecuadorian coast, as illustrated in the Figure 2.1, this basin displays potential for hydrocarbon reserves, highlighted by findings from exploratory drilling. It contains a deep sedimentary fill, with about 10,000 feet of Late Cretaceous deposits atop a Tertiary sequence spanning from Paleocene to Pliocene. The Paleocene to middle Eocene lower Tertiary segments are particularly interesting for hydrocarbon exploration due to the presence of euxinic facies as source rocks and viable reservoir rocks. The basin's structure is mainly defined by block-faulting dynamics, which favor the formation of hydrocarbon traps associated with fault areas over anticlinal structures (Jarrin, 1974).

- **Progreso Basin**

Progreso Basin is in southwestern Ecuador and extending into northwestern Peru, as illustrated in the Figure 2.1, as part of a series of fore-arc basins of pull-apart/translational origin, the Progreso Basin's development and sedimentary infill are deeply entwined with the tectonic interactions between the South American and the Nazca plates. The genesis of this basin during the Oligocene, progressing into the early Miocene, is marked by strike-slip deformation that aligns with the broader tectonic narrative of the region, including the detachment of the Nazca Plate from the South American Plate (Lara-Gonzalo et al., 2019).

2.3 The Esmeraldas-Borbón Basin

Situated along the northern coast of Ecuador, the Esmeraldas-Borbón Basin spans from the northernmost part of Ecuador to the border with Colombia. This single basin, extending predominantly on land between the Mataje and Canande faults, encompasses a geograph-

ical area bounded by the foothills of the Western Cordillera to the east and the Pacific Ocean to the west. Within this basin lies the Horst de Río Verde, effectively dividing the basin into two distinct sub-basins: the Borbón Basin to the north and the Esmeraldas Basin to the south.

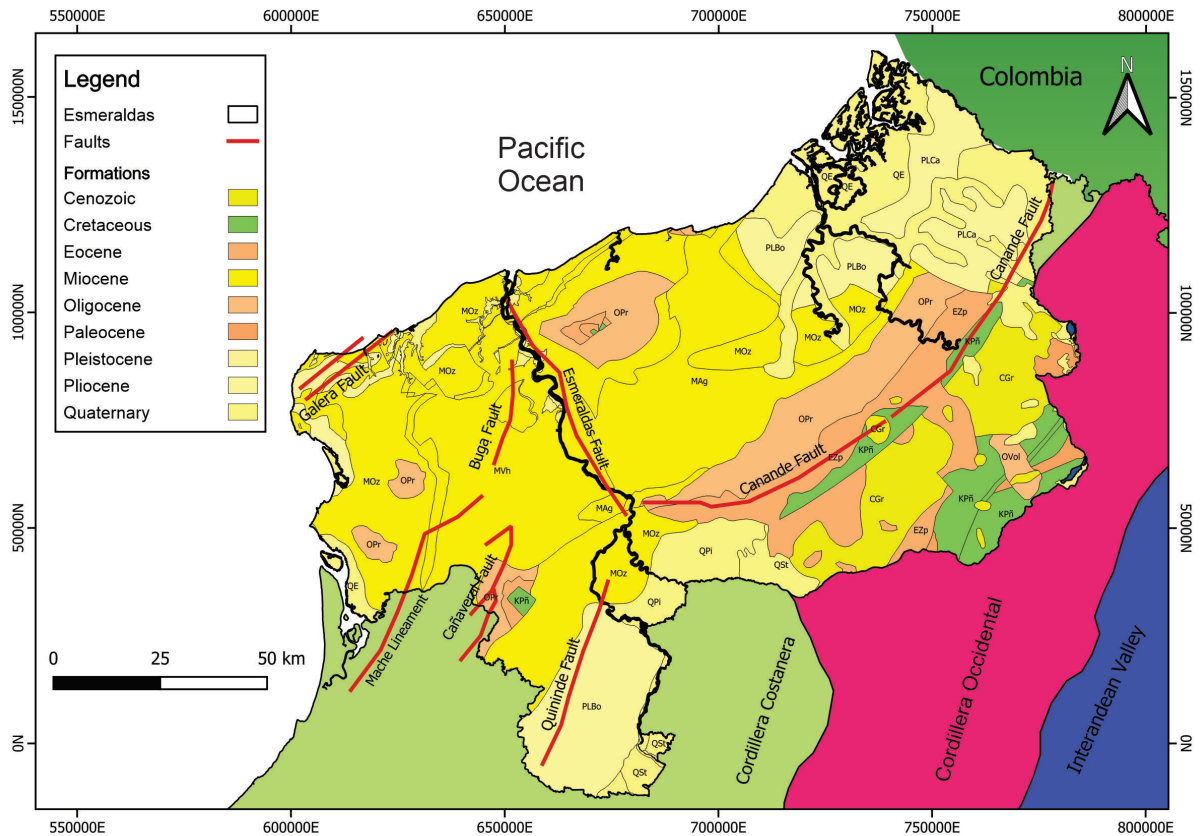


Figure 2.2: Geologic map of the Esmeraldas-Borbón Basin: This detailed representation showcases the geological outcrops of the main formations, as well as the basin’s major geological faults and structures. Based on [Reyes and Michaud \(2012\)](#).

The Esmeraldas-Borbón Basin’s sedimentary successions span from the Cretaceous to the Neogene, reflecting the complex interplay between the Caribbean and South American plates, as illustrate in Figure 2.2. Three phases mark the basin’s evolution: altered extension, quiescence-thermal subsidence along the western side, and pronounced tectonic inversion ([Carrillo et al., 2022](#)). Initially dominated by extensional kinematics from the Late Cretaceous to the Eocene, the basin’s development is a testament to the dynamic geological processes at play.

Significantly, the Late Cretaceous accretion of the Caribbean Large Igneous Province

(CLIP) to the South American margin has profoundly influenced the basin's structure and stratigraphy. The underlying basement consists of mafic rocks from an oceanic plateau, crucial to the Pallatanga and Piñon blocks. Above these, Paleocene-Eocene successions record detrital inputs from continental and volcanic arc sources (Vallejo et al., 2019).

Stratigraphically, the basin features Cretaceous to Miocene clastic deposits, highlighting sustained volcanic influence from the Andean magmatic arc. The accretion of the Piñon and Pallatanga blocks around 73 Ma has significantly shaped the tectonic landscape of southwestern Ecuador and northwestern Peru, contributing to a complex Cenozoic forearc development (Aizprua et al., 2019).

The stratigraphic encompasses a diverse range of clastic deposits, evidencing the basin's dynamic geological evolution under the influence of sustained volcanic activity and the shifting tectonic forces of the Andean magmatic arc. The stratigraphy is marked by significant depositional sequences that chronicle the interplay between tectonic terrane accretion and the sedimentary processes that have sculpted the basin's current geological framework. Notably, the accretion of the Caribbean Large Igneous Province (CLIP) to the South American margin has left a profound imprint on the basin's stratigraphic profile, introducing mafic materials from an oceanic plateau into the sedimentary cycle. These sequences, underpinned by a foundation of Paleocene-Eocene successions and detailed by inputs from both continental basement rocks and igneous material from volcanic arcs, provide crucial insights into the basin's depositional history and its potential resource distribution (Vallejo et al., 2019; Aizprua et al., 2019).

The basin's numerous geological structures, including faults and folds, underscore its complex history influenced by Andean orogeny, volcanic activity, and sedimentary processes. The Canande, Tanigüe, and Esmeraldas Faults, along with a central dome and primary folds, play pivotal roles in the basin's tectonic framework. These structures not only reveal the basin's dynamic evolution but also its potential for hydrocarbon and mineral exploration, indicating significant economic importance.

Chapter 3

Database and Methodology

3.1 Database

The focus of this research is the Borbón-Esmeraldas Basin, located in the northern coastal region of Ecuador. Given the sensitive nature of our data and the confidentiality clauses binding our study, we are restricted from disclosing the coordinates of the study area, seismic lines, and well-log. Nevertheless, our research encompasses an expansive area of 3832.706 km^2 , predominantly spanning the central and significant segments of the Borbón-Esmeraldas Basin.

Our initial literature survey has been fruitful, unearthing a wealth of geological, lithological, biostratigraphical, and structural insights from preceding inquiries, Which helped reconstruct the Chapter 4. These valuable findings have laid a robust foundation for our work, enabling us to forge ahead with an intricate seismic interpretation. This progression is notably achieved despite the challenge posed by the absence of detailed reservoir characterization data. Our meticulous approach aims to unravel the complexities of the basin's subsurface structures.

In the pursuit of understanding the complex subsurface geological structures and stratigraphy of the northern Ecuadorian coast, this study leverages a comprehensive suite of geophysical tools and datasets. Central to our exploration are seismic lines and well logs, which together form the backbone of our investigative methodology, and will be detailed below:

3.1.1 Seismic lines

Seismic lines are fundamental tools in the exploration and characterization of subsurface geology, serving as the backbone for seismic surveys. These surveys generate detailed images of the stratigraphic sequences and structural features beneath the Earth's surface, providing invaluable data for interpreting geological formations, identifying potential hydrocarbon reservoirs, and understanding tectonic activities. By sending acoustic waves into the ground and analyzing their reflections off various geological interfaces.

El Ministerio de Energía y Recursos Naturales No Renovables has diligently assembled seismic data relevant to the northern Ecuadorian coast. This dataset spans an extensive 3832.706 square kilometers and comprises critical information derived from eleven seismic lines of which five lines extend in the SW to NE direction, and six lines that cross perpendicularly extend from SE to NW, forming a grid area., as show in the Table 3.1, and Figure 1.1. Reprocessed in prior investigations, the seismic data chronicles a broad historical span from the Piñon Formation, dating back roughly 90 million years, to the more recent Upper Onzole Formation, approximately 5 million years old. This wide temporal scope is crucial for a detailed understanding of the basin's geological evolution.

Table 3.1: Seismic Line Catalog: this table provides a detailed inventory of the seismic lines analyzed within the area of this study, the location of the seismic lines is shown in Figure 1.1.

Survey Management (Seismic Lines SW-NE)
1A
2A
3A
4A
5A
Survey Management (Seismic Lines SE-NW)
5B
7B
8B
9B
10B
11B

3.1.2 Well log

Well logs are indispensable tools in the geosciences, offering a direct measurement of the physical properties within boreholes. These detailed records are obtained by lowering logging tools into boreholes to measure various parameters such as resistivity, porosity, density, and lithology, among others. The data acquired from well logs provide a continuous profile of the subsurface conditions, facilitating the interpretation of geological formations, assessment of reservoir potentials, and determination of hydrocarbon saturation.

Central to this research is the Borbón-1 well log, a comprehensive dataset that is instrumental in understanding the subsurface geological conditions of the Borbón Esmeraldas Basin. Reaching depth of approximately 3,000 meters. The Borbón-1 well log is rich in a variety of data types, including Lateral Natural (LN), Spontaneous Natural (SN), Spontaneous Potential (SP), and P-wave velocity (Vp). This well log is invaluable for delineating the subsurface geological framework of the basin, offering detailed insights into its structural and stratigraphic complexities. The Telembí-1 well log, that has less information because it only has a depth of 1300 meters, contributes additional context to the study but does not encompass the range of data types found in the Borbón-1 log, as shown in the Table 3.2:

Table 3.2: Well-Log Data of Borbón-1 and Telembí-1: This table compiles data from two wells, including measurements of Natural Gamma Ray (LN), Spontaneous Potential (SP), Sonic Neutron (SN), P-wave velocity (Vp), and Resistivity (RES), and N/A is Not Applicable. Each column represents a distinct well log used to characterize subsurface geological formations. The location of the well-logs is shown in Figure 1.1

Record/Data	Borbón-1	Telembí-1
LN (Porosity %)	[Data de LN]	N/A
SN (us/ft)	[Data of SN]	N/A
SP (mV)	[Data of SP]	[Data of SP]
Vp (ft/s)	[Data of Vp]	N/A
RES	N/A	[Data of RES]

The compiled seismic data was systematically loaded into Kingdom software, which was developed by Seismic Micro-Technology (SMT), a part of IHS Markit. Kingdom is acclaimed for its proficiency in seismic and geological interpretation, equipped with specialized modules, advanced visualization tools, in-depth analysis capabilities, and robust characterization features. This software plays a key role in the interpretation and analysis

of the seismic data of this thesis, contributing to a more nuanced understanding of the basin's stratigraphy.

3.2 Methodology

The methodology implemented in this thesis diverges from conventional approaches by integrating advanced geophysical and geological analysis techniques to achieve a comprehensive understanding of the Esmeraldas-Borbón Basin. This integrated methodology encompasses several distinct phases, each designed to build upon the previous, thereby ensuring a detailed exploration of the basin's geological framework. The process begins with the generation of synthetic seismograms and the enhancement of seismic lines, progresses through the creation of time and isopach maps accompanied by petrophysical analysis, and culminates in the interpretation of sequential stratigraphy. This approach facilitates a more accurate interpretation of seismic data, enhancing the identification of key geological features and providing a nuanced understanding of the basin's sedimentary evolution.

The research was conducted in meticulously designed phases to ensure a deep understanding of the geological characteristics of the study area. The initial phase involved gathering bibliographic information to understand the geological context of the area. This data collection encompassed geological, lithological, biostratigraphic, and facies aspects, this information comes mainly but not only from the book *Micropaléontología Ecuatoriana* by [Ordoñez et al. \(2006\)](#). Such comprehensive insight will enhance understanding of the region and enable a more accurate interpretation of the sequential stratigraphy based on seismic data. The next phase involved improve the quality of seismic lines and generating synthetic seismograms. This crucial step was imperative for calibrating the seismic well tie, significantly improving the accuracy of seismic interpretations by clearly delineating critical features such as faults and stratigraphic horizons of interest.

Subsequently, the study progressed to the generation of time maps and isopach maps, accompanied by a thorough analysis of petrophysical properties, and geohistorical graphs. These processes were instrumental in evaluating the spatial distribution of geological layers and their physical characteristics.

The research culminated in the interpretation of the area's sequential stratigraphy, in-

tegrating all the preceding steps. This holistic approach enabled a comprehensive analysis, merging seismic data with petrophysical findings and stratigraphic mapping to precisely delineate depositional sequences. This methodology facilitated a deeper understanding of the temporal and spatial evolution of the sedimentary environment. The complete methodology is detailed by steps in Figure 3.1.

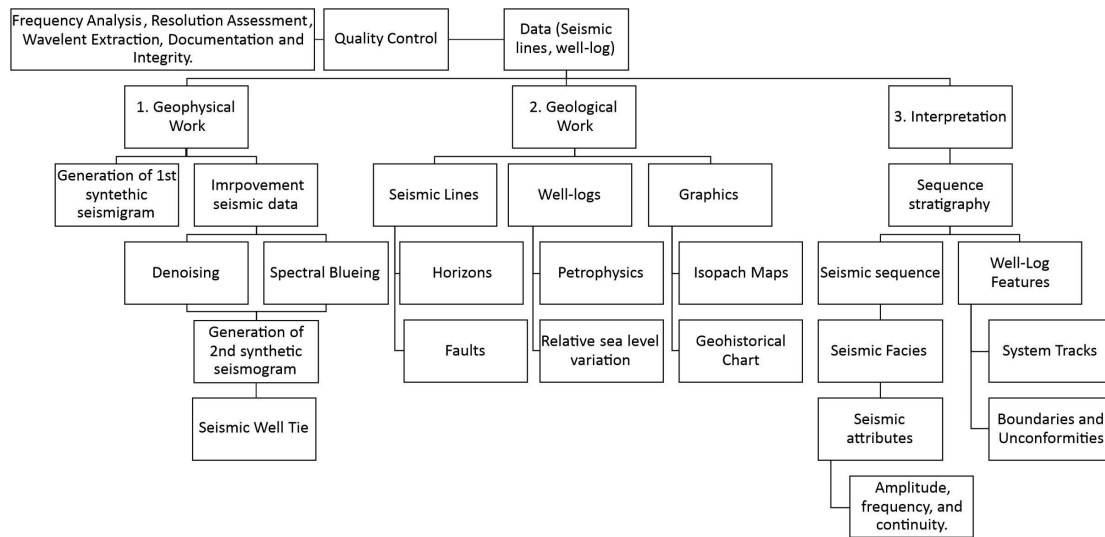


Figure 3.1: Schematic Overview of the Research Methodology: This figure provides a schematic representation of the research methodology, detailing the sequential steps and processes from the study's inception through to its conclusion.

3.2.1 Quality Control

In this thesis, we have applied a meticulous quality control methodology to the seismic data, utilizing Kingdom Software as the primary tool for analysis. This approach focused on evaluating frequency, resolution, and wavelet extraction, which are three essential elements for enhancing the quality of seismic data. This quality control was based on two studies: *Seismic Data Analysis: Processing, Inversion, and Interpretation of Seismic Data* of [Yilmaz \(2001\)](#), and *Offset-dependent reflectivity: Theory and practice of AVO analysis* of [Castagna and Backus \(1993\)](#) used for wavelet extraction. By applying this methodology to our dataset, we ensured a comprehensive optimization of seismic data quality, pivotal for accurate geological interpretation and analysis.

- Frequency Analysis

The initial phase involved spectral analysis tools within Kingdom Software to scrutinize the frequency content of the seismic data. The aim was to pinpoint dominant frequencies and evaluate the bandwidth, foundational for understanding the resolution and interpretability of seismic images. This frequency analysis is vital for confirming the presence of adequate frequency components to discern geological details of interest, thereby enhancing the quality and utility of seismic interpretations.

- Resolution Assessment

Subsequent to frequency analysis, the methodology emphasized the resolution assessment of the seismic dataset. This step entailed a thorough examination of both vertical and lateral resolution capabilities, crucial for the delineation of closely spaced geological strata. The resolution's dependency on frequency content necessitated this analysis to define interpretation boundaries and set realistic expectations about the detail level achievable from the seismic data.

- Wavelet Extraction

The concluding stage entailed extracting wavelets from the seismic data, a pivotal process for synthesizing seismograms that facilitate seismic-well ties. Utilizing Kingdom Software, representative seismic traces were selected for their clarity and minimal noise interference to derive a wavelet reflective of the seismic source and recording system. This extraction ensures synthetic seismograms' alignment with actual seismic data, enhancing the correlation accuracy between seismic reflections and well-log information.

- Documentation and Integrity

Throughout the quality control process, meticulous documentation of each step was maintained, providing a thorough record of the techniques and analyses employed. This documentation not only upholds the thesis's integrity but also serves as a valuable resource for future research employing similar methodologies or datasets. The diligent application of these quality control measures via Kingdom Software is integral to the success of the thesis's seismic interpretation and analysis endeavors.

3.2.2 Generation of Pseudo-Sonic Logs

The generation of pseudo-sonic logs is a crucial technique for geophysical exploration, especially when sonic records are not available. The process usually involves the application of the Faust equation, which relates seismic wave velocity to other measurable properties like depth and resistivity. This method has been adapted and applied in various geophysical studies to estimate sonic logs when they are not available.

As highlighted in the preceding section, the two wells situated within the study area lack sonic records. Consequently, to bridge this data gap, it became imperative to synthesize pseudo-sonic records. This synthesis was achieved by applying the Faust Equation (Faust, 1951) to wells located to the south of the study area: Ricaurte, Chone, and Calceta.

$$V \equiv a \times (Z \times R)^{\frac{1}{m}} \quad (3.1)$$

V is the speed with which the compressional wave travels in the formation, obtained from the transit time from the real sonic log, Z is the depth, and R is the resistivity (ILD and LLD) available in each well. To find the parameters of “a” and “m” in each well, it is necessary to linearize equation 3.1, obtaining the following equation:

$$\ln(V) = \ln(a) + \frac{1}{m} \times \ln(Z \times R) \quad (3.2)$$

Or also:

$$V' = A' + M' \times (Z \times R)' \quad (3.3)$$

This transformation was applied to the well data, and cross graphs of $\ln(V)$ and $\ln(Z \times R)$ were constructed, as show in Figure 3.2, then linear regression was applied to obtain the values of A' and M' where:

$$A' = \ln(a) \quad (3.4)$$

and,

$$M' = \frac{1}{m} \quad (3.5)$$

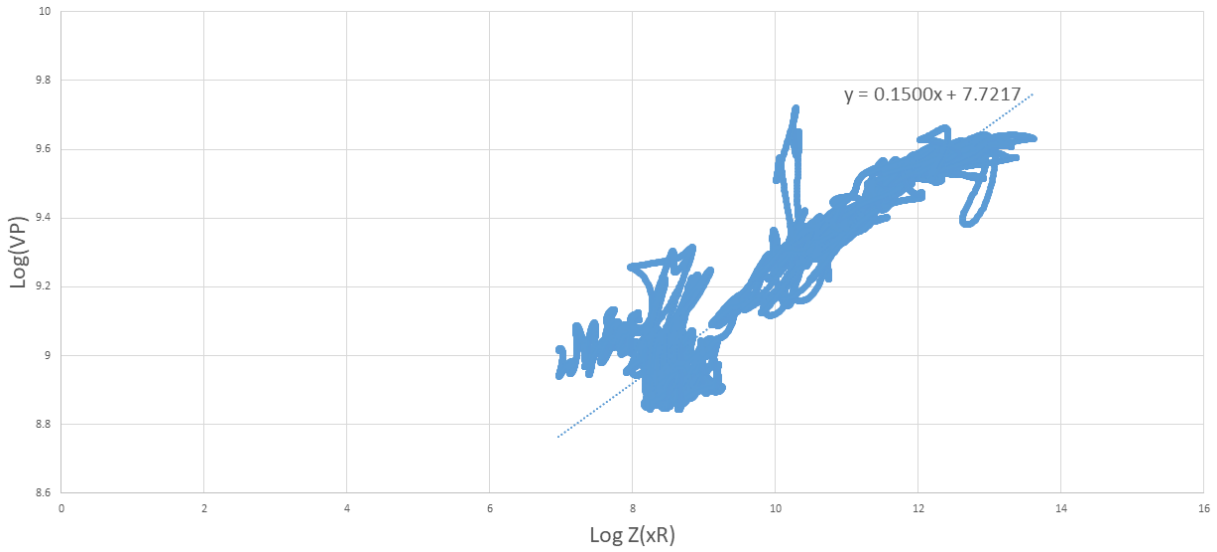


Figure 3.2: Linearization of $Z \times R$ vs. V_P for determining constants a and m : This figure presents the linear relationship between the product of impedance (Z) and resistivity (R) plotted against P-wave velocity (V_P), utilized to identify the constants a and m . The graph demonstrates the method for extracting these constants, crucial for quantifying the geological and petrophysical parameters of the subsurface formations.

Returning the changes that were made when linearizing the equation gives:

$$a \equiv e^A \quad (3.6)$$

and,

$$m \equiv \frac{1}{M} \quad (3.7)$$

In the three wells, similar values were found within the constants m and a . These constants were used to generate a pseudo-sonic record from the following equation:

$$DT_P \equiv \frac{1}{V} \equiv \frac{1}{a} \times (Z \times R)^{\left(-\frac{1}{m}\right)} \quad (3.8)$$

where DT_P is a generated pseudo-transit time. Finally, to determine which of these pseudo-sonic will best reproduce the shape of the real sonic, a graphic comparison was made where DT_1 (Ricaurte) was the pseudo-sonic record that best reproduced the shape of the real sonic in all wells with a coefficient correlation of 0.939, as show in the Figure 3.3.

The initial step involves converting depth-based well-log data into the time domain,

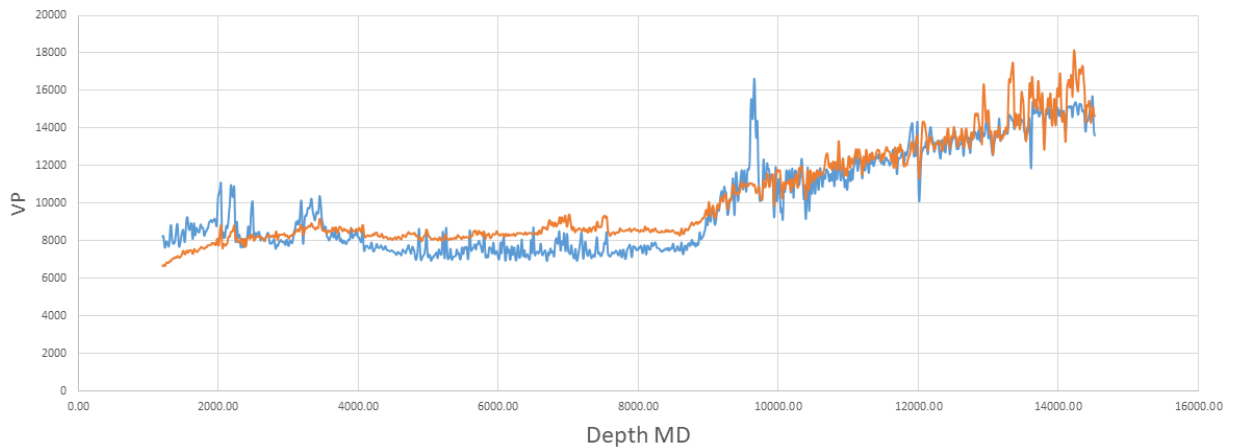


Figure 3.3: Comparison of Real VP Records (Blue) with Pseudo-Sonic Log (Orange): This figure illustrates a side-by-side comparison of actual P-wave velocity (VP) records, depicted in blue, against the pseudo-sonic log data, shown in orange. It visually contrasts the measured VP values from well logs with those derived from the pseudo-sonic methodology, highlighting the accuracy and discrepancies between these two approaches in evaluating subsurface velocities.

crucial for correlating with time-domain seismic data. This is achieved by establishing a time-depth relationship using velocity logs. Following this, a wavelet representing the seismic source signature is generated or extracted from seismic data, based on the availability and quality of seismic data.

Acoustic impedance modeled from the well logs is then used to calculate a reflectivity series, reflecting the impedance contrasts at geological interfaces. The process culminates in the convolution of the wavelet with the reflectivity series, producing the synthetic seismogram. This seismogram simulates the seismic response of subsurface layers, as interpreted from well-log data.

The synthetic seismogram is then analyzed and compared with actual seismic data to validate the seismic interpretation. Adjustments are made to ensure a high fidelity between the synthetic and actual seismic data. Meticulous attention to detail and rigorous quality control measures are maintained throughout the process, using Kingdom Software.

3.2.3 Seismic Well Tie

Once the synthetic seismograms were generated, the next phase involved aligning them with the seismic data. This alignment was a meticulous process, requiring careful matching of the synthetic seismogram's reflections with the corresponding reflections in the seismic

data. The primary goal here was to identify the same geological interfaces in both datasets. Adjustments in time-depth relationships or wavelet characteristics were often necessary to achieve a close match.

The seismic-well tie was then scrutinized for accuracy. This involved a detailed comparison of key seismic events and corresponding log markers. Areas of interest, such as potential reservoir zones or significant geological boundaries, received extra attention to ensure precise correlation. Discrepancies between the seismic and well data were thoroughly investigated, leading to a deeper understanding of the subsurface geology and potentially revealing areas where seismic data processing or interpretation might need refinement.

Throughout the seismic-well tie process, the integration of different data types and the application of rigorous quality control measures were paramount. The aim was to create a reliable and coherent geological model that accurately represented the subsurface. This process, enabled by the powerful tools in Kingdom Software, provided a robust framework for geological interpretation, significantly reducing uncertainties and aiding in more informed decision-making in exploration and development projects.

3.2.4 Seismic Data Improvement

Seismic data acquisition is essential for the exploration and characterization of geophysical basins, enabling the mapping of subsurface structures and resource assessment. Yet, data quality is compromised by noise and high-frequency signal attenuation, affecting seismic image clarity. Overcoming these challenges necessitates advanced techniques like noise removal (denoising) and spectral blueing. Denoising aims to eliminate noise while preserving relevant signals, and spectral blueing enhances high-frequency signals to improve seismic image resolution, enabling more accurate data interpretation.

Key research in this field includes DeepDenoiser by [Zhu et al. \(2018\)](#), which uses deep neural networks for efficient seismic denoising, and a study by [Kazemeini et al. \(2008\)](#) demonstrating seismic resolution improvement through spectral blueing. These advancements highlight the potential of sophisticated techniques in optimizing geophysical basin interpretation.

Our study underscores the critical need for applying denoising before spectral blueing. This sequence is crucial as noise can obscure or distort the high-frequency signals targeted

by spectral blueing. Removing noise first clarifies the signal, allowing spectral blueing to more effectively enhance the signal's true characteristics. This approach significantly improves seismic image resolution and quality, leading to a more detailed and accurate geophysical interpretation. This was achieved through various tests within the lines mentioned in Table 3.1.

- **Denoising**

The methodology adopted for seismic data enhancement emphasized Denoising as a pivotal step to markedly improve the quality of the seismic lines and previous step to Spectral Blueing. This approach commenced with the categorization of seismic noise into three primary types: random, coherent, and acquisition-related. To tackle random noise, statistical methods such as median and Wiener filtering were utilized. In contrast, coherent noise, characterized by more uniform patterns, was addressed using predictive filtering techniques. Additionally, issues related to acquisition, like irregular sampling, were managed through the deployment of advanced 3D interpolation methods. A critical element of this strategy was the introduction of Noise2Void (N2V), a novel technique especially useful in scenarios lacking clean, noise-free training data, as shown in Figure 3.4. Leveraging the principle of predicting noise from the surrounding pixels and training on the noisy data itself, N2V emerged as a highly versatile component in the denoising toolkit, significantly enhancing the seismic data's overall quality and interpretability without reliance on traditional, noise-free reference data.

- **Spectral Blueing**

The methodology for enhancing seismic data through Spectral Blueing encompassed a structured approach, aimed at counteracting the common attenuation of high-frequency components that often results in diminished resolution. The procedure involved the development and application of custom algorithms, initiating with the transformation of seismic data from the time domain to the frequency domain via Fourier transform. This crucial step facilitated direct manipulation of the data's frequency spectrum.

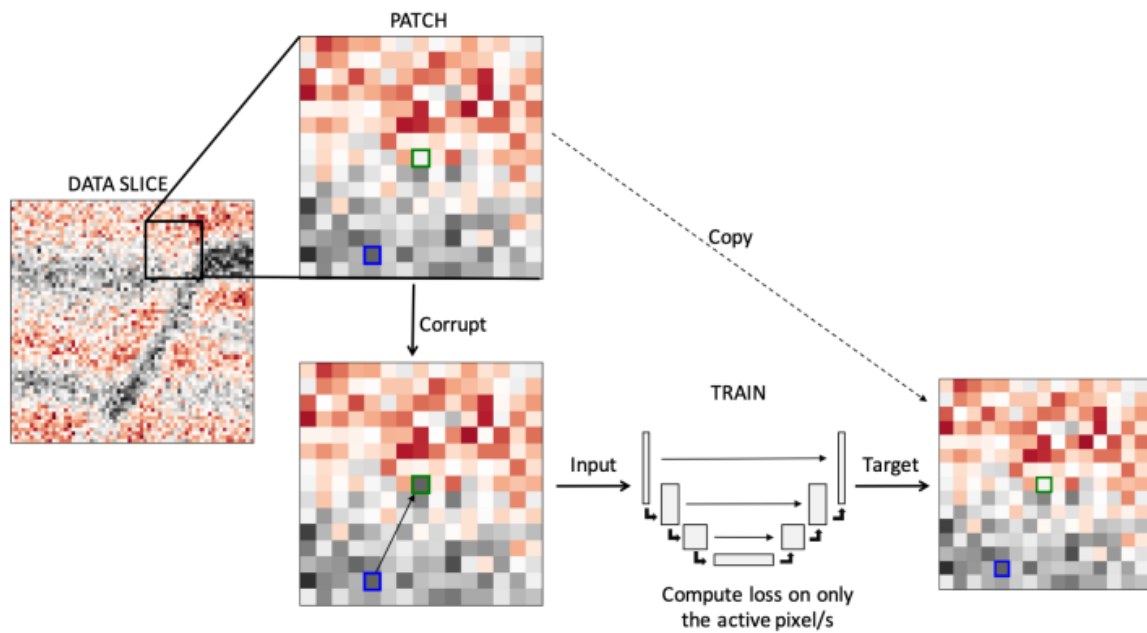


Figure 3.4: Schematic Illustration of the Noise2Void Denoising Procedure: This diagram depicts the step-by-step process of the Noise2Void technique for removing noise from images without the need for clean training data. By intelligently sampling pixels and predicting their values based solely on the surrounding pixel information, the algorithm effectively reduces noise while preserving the integrity of the original image content (Birnie et al., 2021).

In the frequency domain, a bespoke filter was applied to selectively augment higher frequency components. The design of this filter, including the degree of amplification and targeted frequencies, was meticulously tailored based on an initial analysis of the data's frequency spectrum and specific enhancement goals. Following this, an inverse Fourier transform was employed to revert the data back to the time domain, completing the Spectral Blueing process.

This technique was thoroughly evaluated by comparing the enhanced seismic data against the original, with a focus on resolution improvement and the enhanced interpretability of geological features.

These methodologies have been exceptionally effective in diminishing both random and coherent types of noise, which typically obscure geological signals vital for precise subsurface analysis. Random noise, originating from a variety of environmental conditions and equipment or processing inaccuracies, along with coherent noise like multiples and ground roll, greatly interfere with the clarity of seismic reflections that are crucial for

understanding geological formations.

3.2.5 Second Synthetic Seismogram and Seismic Well Tie

The methodology for the advanced stage of the thesis involved two main processes: the creation of a second synthetic seismogram using enhanced seismic data and the execution of seismic-well ties to evaluate the correlation between these data and well log information, both guided from [Yilmaz \(2001\)](#). The enhanced seismic data, improved through Spectral Blueing and denoising techniques, provided a foundation for generating the second synthetic seismogram. This involved convolving a refined seismic wavelet, derived from the improved seismic dataset, with the reflectivity series obtained from well logs, aiming for a synthetic seismogram that more accurately mirrors actual seismic data for better well seismic tie.

The seismic-well tie process then aligned this second synthetic seismogram with the enhanced seismic data to accurately map geological features from well logs to their seismic counterparts. The effectiveness of this alignment was quantified using the correlation coefficient, a statistical measure of similarity between the synthetic seismogram and the seismic data. A high correlation coefficient would indicate a successful match, demonstrating that the seismic reflections accurately represent the geological layers documented in the well data, as illustrated in Figure 3.5.

3.3 Seismic Interpretation

In the conducted study, a comprehensive methodology was employed to interpret seismic data, effectively integrating semi-automatic tracking with manual corrections. Key stratigraphic horizons, namely Piñon, Zapallo, Pambil, Viche, Angostura, and Upper Onzole, were identified within the seismic lines based on amplitude characteristics. The semi-automatic capabilities of Kingdom Software facilitated initial horizon picks, which were then meticulously extended across the seismic dataset, leveraging the software's ability to maintain amplitude and phase continuity.

For regions where seismic reflections were unclear or interrupted, a rigorous manual correction process was undertaken. This ensured horizon picks were accurately aligned with

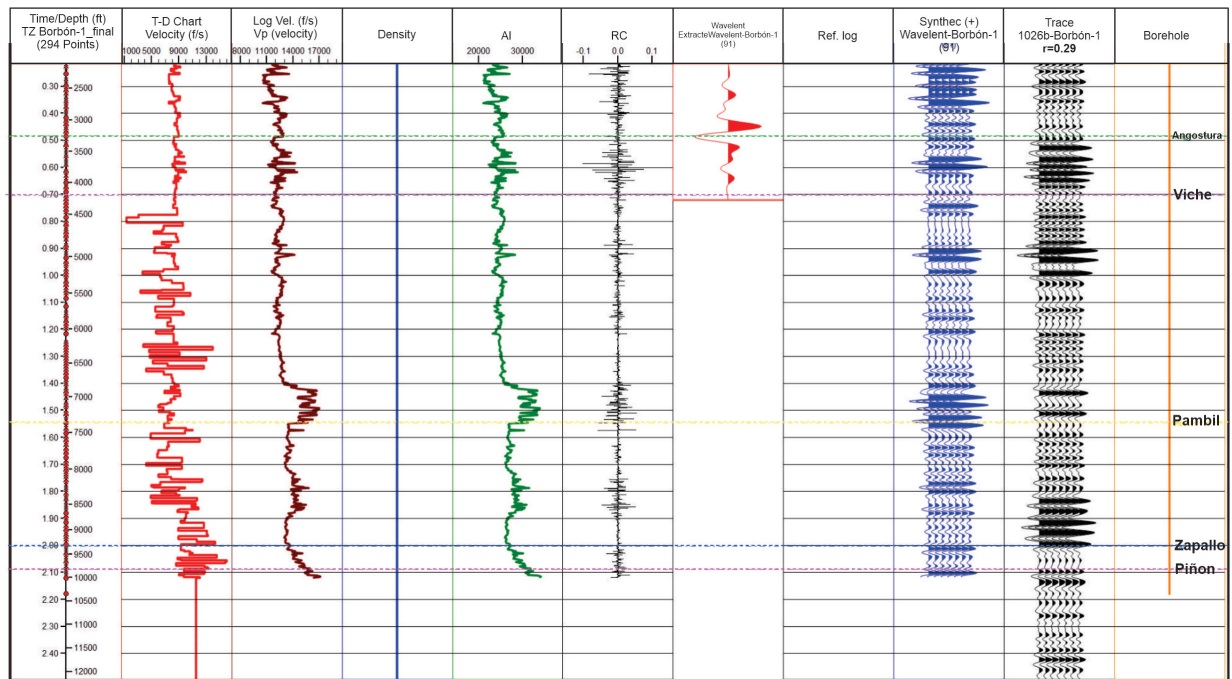


Figure 3.5: Second Synthetic Seismogram with Wavelet Post-Seismic Data Improvement and Final Well-Seismic Tie. This figure depicts the second iteration of a synthetic seismogram, incorporating an optimized wavelet based on refined seismic data. Including the correlation coefficient ($r = 0.29$) that improved compared to the first synthetic seismogram.

true seismic reflections or manually traced where automated methods proved inadequate. The documentation and extension of these horizons across additional seismic lines ensured thorough mapping and correlation throughout the study area.

Additionally, the manual identification of geological faults was performed, focusing on faults visibly discernible within the seismic lines. This step provided a detailed representation of geological discontinuities, enhancing the study's interpretation of the subsurface geological structure, as shown in Figure 3.6.

Moreover, isopach maps of key sequences were meticulously crafted. Alongside these, geohistorical charts were also developed to facilitate a comprehensive analysis of subsidence.

3.3.1 Depositional Sequences and Sedimentary Framework

All seismic lines underwent a seismic-to-well tie, as demonstrated in the previous section, enabling the effective alignment of seismic lines with well log data. In these profiles, to understand the factors controlling sedimentation, structural features and significant depositional sequences were identified and mapped. The depositional sequences were charac-

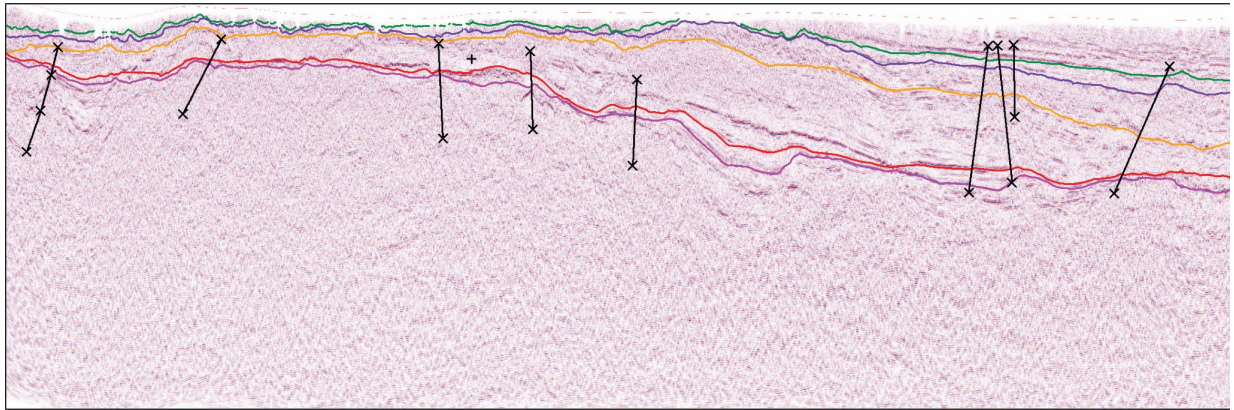


Figure 3.6: Seismic Line 3A: *Color-Coded Horizon Interpretation* - Horizons are distinctly marked for clarity: Piñón in purple, Zapallo in red, Pambil in yellow, Viche in blue, and Angostura in green. Interpreted faults are delineated in black, providing a comprehensive visual guide to the geological structure.

terized through visual analysis of reflector properties such as amplitude, continuity, and frequency, and by comparing trace counts to assess the timing and configuration of seismic reflections.

The composition of the depositional sequences was determined through lithologic characterization of well data, resulting in eight lithostratigraphic sections (Sections A to H). These sections were enhanced with information from previous studies. To showcase lateral sedimentation patterns, a stratigraphic correlation incorporating this data was developed.

3.3.2 Isopach Maps

The methodology for this geological study entailed a structured approach to subsurface analysis using Kingdom Software, focusing on predefined geological horizons: Zapallo, Pambil, Viche, and Angostura. Initially, time maps for the upper and lower boundaries of these layers were generated, establishing the foundation for calculating the time thickness, or isochron, by subtracting the seismic time of the upper horizon from the lower.

This calculation process was conducted for each of the horizons, serving as a crucial step in approximating the physical thickness of geological layers, under the assumption of consistent seismic velocity. The next phase involved transforming this seismic time thickness into actual geological thickness to construct isopach maps. This conversion, utilizing an average seismic velocity, accurately reflected the physical thickness of the sedimentary layers for Zapallo, Pambil, Viche, and Angostura.

Each isopach map produced provided a detailed visualization of layer thickness variations, assisting in the geological interpretation and analysis of depositional environments

3.3.3 Geohistorical graphics

To create a Geohistorical Graph, one must first define the total subsidence, denoted as H . The value of H is calculated for predetermined time intervals, expressed as $(T_0 - T_n)$. These intervals represent significant epochs or stages in the geological timeline, capturing the beginning T_0 and the end T_n of the subsidence event.

The calculated subsidence H is directly related to the slope of the graph (Figure 3.7), we rely mainly on the calculation notes of [Allen and Allen \(2013\)](#). In mathematical terms, the slope is the rate of change of subsidence with respect to time, which can be expressed as:

$$\text{Slope} = \frac{\Delta H}{\Delta T} = \frac{H(T_n) - H(T_0)}{T_n - T_0} \quad (3.9)$$

where ΔH is the change in subsidence and ΔT is the change in time from T_0 to T_n . The steeper the slope, the greater the rate of subsidence during that particular interval.

The evolution of the Borbón-Esmeraldas Basin was traced using geohistorical graphs, starting with gathering data from Borbón-1 and Telembí-1 well-logs and literature on sediment characteristics. This information was enhanced by applying standard parameters for initial porosity, compaction, and sediment density ([Gallagher and Lambeck, 1989](#)), along with paleobathymetry estimates from facies analysis. This data was analyzed and synthesized with global sea level changes [Haq et al. \(1987\)](#), allowing for a detailed reconstruction of the basin's development and the correlation between local and global geological phenomena. The graph's scale and format were tailored to clearly present these insights.

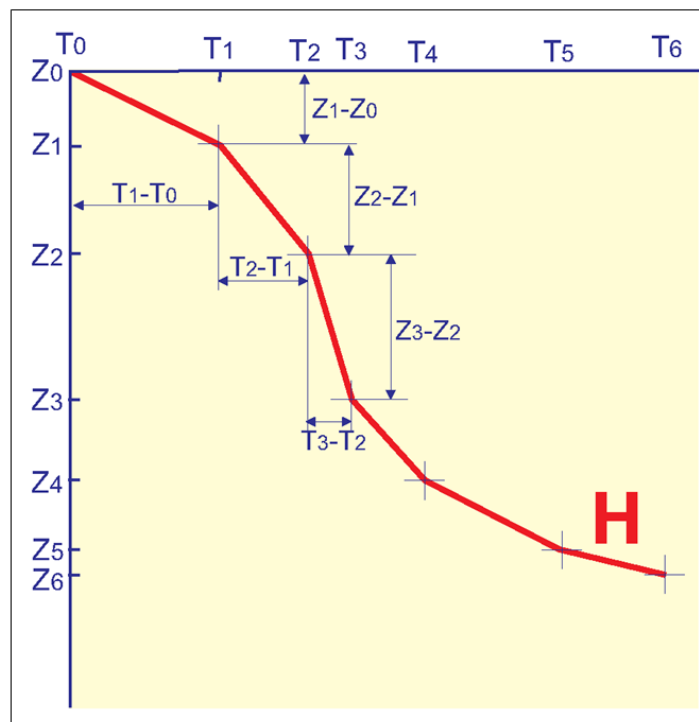


Figure 3.7: Geohistorical Graph Illustrating Subsidence: This graph represents total subsidence, denoted as H, with specified time intervals ($T_0 - T_n$) and Z representing depth.

Chapter 4

Stratigraphy of the Borbón Esmeraldas Basin

Savoyat et al. (1970) suggest that the Esmeraldas-Borbón Basin can be schematically divided into three areas (Figure 4.1): a western zone (WZ), corresponding to the Esmeraldas Basin; a central elevated zone (CZ), featuring the Punta Ostiones, Río Verde, and Río Cube Horsts; and a subsiding northeastern zone (NZ) that forms the Borbón Basin:

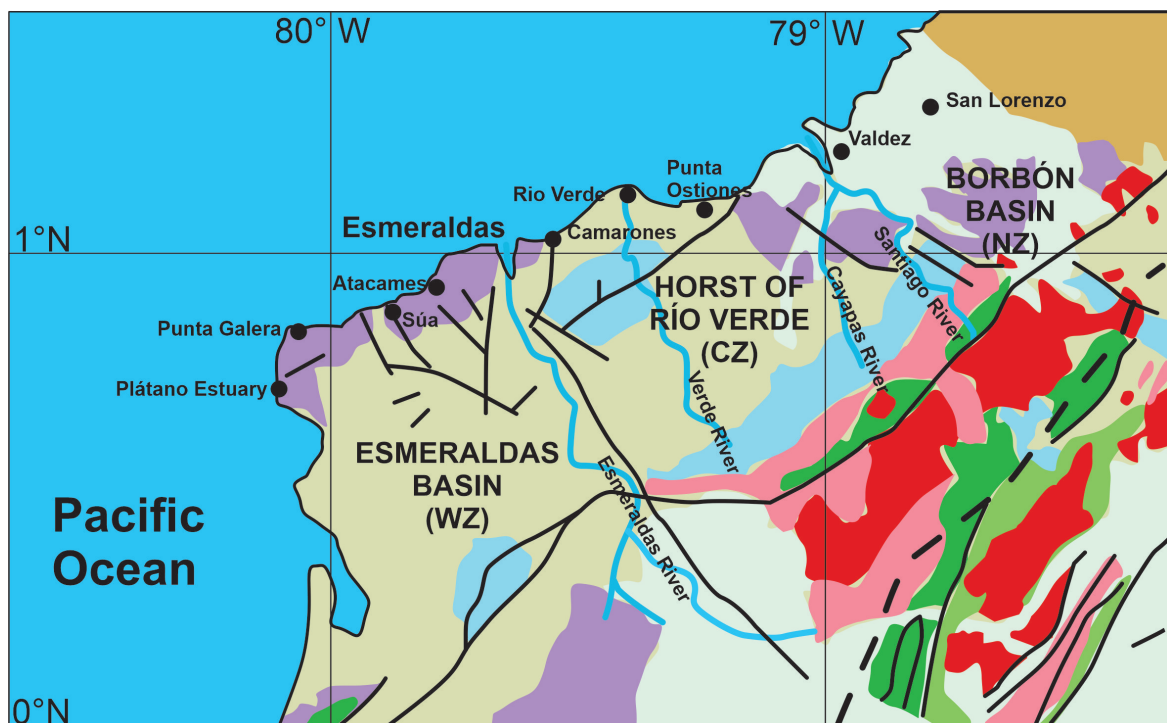


Figure 4.1: Outline of the distinct areas within the Esmeraldas Borbón Basin including: a) the West Zone (WZ), b) the Elevated Central Zone (CZ), and c) Northeast Zone (NZ). Based on the map of Ordoñez et al. (2006)

Western Zone: The Muisne Mountains feature a shallowly marked synclinal axis running W-SW to E-NE, with a depth reaching up to 2500m. Towards the west, the basement rises, forming a subtly defined anticlinal structure (Figure 4.1).

Central Zone: This area represents a high, faulted region where ancient sediments are exposed (Figure 4.1).

- At Punta Ostiones, limestone from the Ostiones Formation underlies the Pambil Formation.
- The Río Verde Horst displays complex tectonics, exposing the Piñón, Cayo, Ostiones, and Zapallo formations. Around the Horst, the basal Pambil Formation forms a halo over a large, slightly elevated area upon which the Viche Formation is deposited.
- In the Río Cube Horst, located to the south of this elevated zone, the Piñón, Zapallo, and Pambil formations are exposed.

Northeastern Zone: The Borbón Basin, positioned north of a NW-SE trending fault that bounds the elevated area, is a subsiding zone with a SW-NE axis. It continues the Chagui Basin from southern Colombia. Savoyat and colleagues believe that the Borbón transgression extensively filled the synclinal core and reached the basement in the northern part. Its stratigraphy has been among the most extensively studied by foreign researchers (Figure 4.1).

4.1 Lithostratigraphy

The stratigraphic profile of the Borbón-Esmeraldas Basin has been comprehensively defined through prior studies (Luzieux, 2007; Benitez, 1995; Evans and Whittaker, 1982), revealing a sequence of nine distinct geological formations. These formations are ordered from the oldest at the base to the youngest at the top, in ascending order: the Piñón Formation, Santiago Formation, Zapallo Formation, Punta Ostiones Member, Playa Rica Formation, Pambil Formation, Viche Formation, Angostura Formation, Onzole Formation, Súa Member, and Borbón Formation. This ordered arrangement is depicted in Figure 4.2, providing a visual representation of the basin's geological framework and the temporal succession of its sedimentary units. Below is a brief lithostratigraphic review of each formation:

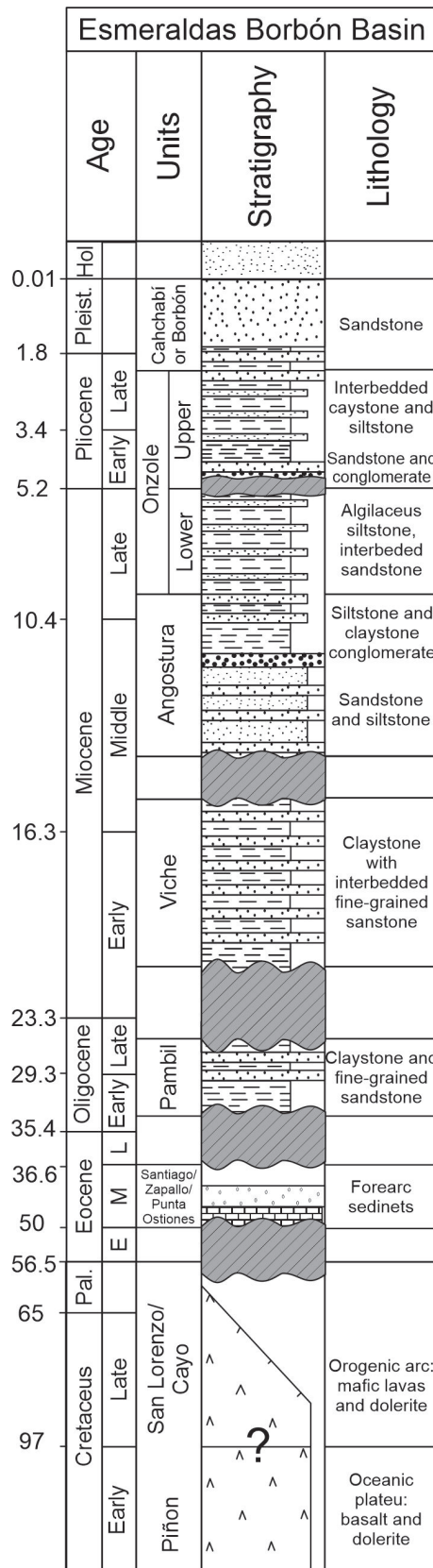


Figure 4.2: Generalized Stratigraphic Column of the Esmeraldas-Borbón Basin: Show principal geological formations and key hiatuses. Based on Jaillard et al. (1997); Deniaud (2000); Marcaillou and Collot (2008); Reyes and Michaud (2012).

4.1.1 Piñón Formation

The exploratory endeavors undertaken by TEXACO-PECTEN, and [Goonses and Rose \(1973\)](#) have furnished insights regarding the basement of the Ecuadorian coast. In Esmeraldas, around 25 km southeast, a few outcrops of Piñón Formation have been identified ([Bristow and Hoffstetter, 1977](#)).

Identified as the basement of the Ecuadorian coast, the Piñón Formation primarily consists of tholeiitic basalts and basaltic andesites, often exhibiting pillow structures ([Jailard et al., 1997](#)). According to [Goonses and Rose \(1973\)](#), these volcanic rocks share a composition similar to those found in oceanic ridges, suggesting an oceanic floor origin. The rocks have been dated to the Late Aptian to Early Albian and the Late Campanian to Maastrichtian.

4.1.2 Santiago Formation

The term for the formation was first introduced by [Olsson et al. \(1942\)](#), with Smith later applying it in a 1947 report for the Telembí Commission. Located in the Borbón Basin, notably at the Santiago River outcrops, it extends over about 500 meters of the stratigraphic column. This formation rests unconformably atop the Piñón Formation, transitioning gradually and conformably to the Zapallo Formation above. Characterized by predominantly fine to medium grey sandstones with calcareous cement and centimeter-scale stratification, it also features hard, slightly slate-like, predominantly silty shales, ending with coarse sandstone layers.

Outcrops of calcareous sediment from this formation along the Santiago River, in the southern Borbón Basin, overlay the Cretaceous bedrock unconformably, with thickness varying between 100 and 500 meters ([Reyes and Michaud, 2012](#)). According to [Ordoñez et al. \(2006\)](#), these sediments, dating to the continental Eocene, are composed of fine to medium grey sandstones with calcareous cement and hard shales, including a top layer of coarse sandstones. The Santiago Formation has been dated from the Middle to Late Eocene period.

4.1.3 Zapallo Formation

The Formation was initially referenced in unpublished reports by the IEPC and has been delineated along the Zapallo Grande and Santiago rivers, tributaries of the Cayapas River. It overlies the Santiago Formation, with outcrops exceeding 500 meters in thickness.

The Zapallo Formation is composed of marine sediments including greenish-grey limonites when fresh, sandstone strata, and tuffs. The formation's thickness variably overlies the Cretaceous bedrock of the Piñón Formation and locally the Santiago Formation. The assigned age for the Zapallo Formation is the Middle to Upper Eocene period (Ordoñez et al., 2006).

4.1.4 Pambil Formation

Defined by geologists from the IEPC in 1947 along the Pambil River where it locally outcrops, though it is also intersected by the Cayapas and Santiago rivers. The formation comprises interbeddings of greenish-grey silty shales when fresh and fine-grained sandstones, with the sandstones and tuff layers being sporadic (Evans and Whittaker, 1982). The determined age for the sediments exposed along the Santiago River is Middle Oligocene, while exposures along the Río Verde correspond to Late Oligocene (Ordoñez et al., 2006).

4.1.5 Viche Formation

It reaches nearly 1000 meters in thickness on both flanks of the Río Verde. Initially defined by geologists from the IEPC in 1946 and 1947, this formation was found on both flanks of the Río Viche, about 10 km from its confluence with the Río Esmeraldas and 40 km SSW of the city of Esmeraldas.

Characterized by calcareous silty shales varying in color from green to dark brown when fresh, with occasional thin tuff layers. The assigned age for this formation is Late Oligocene to Middle Miocene (Ordoñez et al., 2006).

4.1.6 Angostura Formation

Located along the Santiago River in the Borbón Basin, near the confluence of the Río Esmeraldas, this formation is overlain unconformably by the Viche Formation to the north and by the Piñón and Cayo Formations to the south. It comprises coarse to fine-grained

sandstones with a thickness of approximately 35 meters near the Río Esmeraldas and transitions to the Onzole Formation's shales. The assigned age for this formation is Middle Miocene (Ordoñez et al., 2006).

4.1.7 Onzole Formation

Distinguished by two members, the lower part defined by the top of the Angostura Formation and the base of the Súa Member, and the upper part including the Súa and Estero Plátano Members (Evans and Whittaker, 1982). It consists of weathered limonites turning yellowish-brown, with sandstone belonging to the members. For the Onzole Formation, the dated age range is from the Late Miocene to the Pliocene (Ordoñez et al., 2006).

Lower Onzole

Comprised of well-stratified limonites with thin layers of fine-grained sandstone, presenting a dark green to gray color when fresh and turning reddish cream when weathered, along with bioclastic sandy gravel. Thickness ranges between 300 and 800 meters (Evans and Whittaker, 1982). The Lower Onzole has been dated to the Late Miocene (Ordoñez et al., 2006).

Upper Onzole

Dominantly limolitic sandstones with poor to well-defined stratification, ranging in color from creamy grey to reddish-orange when weathered and dark green to gray when fresh. Thin layers of gravel are common, and the formation extends over 1000 meters in thickness in areas from Camarones to Punta Gorda and from Same to Tonchigüe up to Playa Escondida and Estero Plátano. The Upper Onzole has been dated to the Pliocene (Ordoñez et al., 2006).

Súa Member

Composed of medium to fine-grained, massive to well-stratified orange to yellow sandstones, pebbly sandstone, bioclastic sandstone, layers of limonite, and cross-bedding. The maximum thickness reaches 250 meters, tapering to 10 meters east of the Río Esmeraldas

([Evans and Whittaker, 1982](#)). The Súa Member spans from the Late Miocene to the Early Pliocene ([Ordoñez et al., 2006](#)).

Estero Plátano Member

Characterized by well-stratified intercalations of reddish-brown sandstones and medium to fine green limonites, with an approximate thickness of 300 meters. Calcareous concretions up to 25 cm in diameter are present ([Evans and Whittaker, 1982](#)). The Estero Plátano Member ranges from the Early to Middle Pliocene ([Ordoñez et al., 2006](#)).

4.1.8 Borbón Formation or Cachabí Formation

The Borbón Formation's sandstones, also known as the Cachabí Formation, could not be directly dated from outcrops, though their age is inferred from stratigraphic positioning to range from the Pliocene to the Early Pleistocene. This formation is divided into two members:

Clastic member is characterized by acceptable to medium sandstones that are bluish-gray and occasionally yellowish-brown, interspersed with calcareous macrofossils, and volcanic member comprises tuffs and clays with intercalations of greenish-grey tuffaceous sandstones ([Ramírez, 2013](#)).

The depositional history of the Borbón Formation reflects a regression from a shallow marine environment to a transitional environment. Subsequently, a transgressive event is evidenced in the upper part by the presence of lumachelles, which are facies-correlatable with the Tablazo Formation. This sequence culminates in a regional uplift ([Benitez, 1995](#)).

4.1.9 Alluvial Deposits and Terraces

Defined at different levels within the basins of the Esmeraldas, Atacames, and Santiago rivers. The lower terrace level is the current river course, expanding during the dry season, consisting of coarse pebbles and medium to fine grey sand. Alluvial Deposits and Terraces are dated to the Quaternary period.

4.2 Biostratigraphy

Geologists from CIGG have undertaken several exploratory campaigns in these basins. In 1998, under the PETROPRODUCCIÓN-ORSTON Agreement, biostratigraphic studies were conducted in the Esmeraldas basins and the Río Verde Horst. In 1999, in collaboration with researchers from the Smithsonian Institute, explorations were carried out along the Santiago, Cayapas, and Camarones rivers, as well as in the Punta Verde Horst and the Estero Plátano area, where the sediments have also been subjected to micropaleontological analysis. Currently, these basins remain a focus of ongoing research (Ordoñez et al., 2006).

In the Santiago Fm., the uppermost layers of the sequence are characterized by coarse sandstones, notably incorporating *Discocyclusa* spp., which occasionally forms significant microlumachella structures. The key microfauna comprises benthic foraminifera such as *Lenticulina americana* and *Cibicides pseudoungerianus* (spanning Middle Eocene to Early Miocene), along with planktonic foraminifera *Globorotalia broedermanni* (Early to Middle Eocene) and *Globigerina* sp. Radiolarians present, including *Cryptoprora* aff. *ornata*, *Dictyoprora armadillo*, *Eusyringium lagena*, and *Lychnocanoma bellum*, further elucidate the environmental conditions from the Middle to Late Eocene (Ordoñez et al., 2006).

For Zapallo Fm., in the Río Verde Horst, samples taken from both flanks of the anticline exhibit a diversity of radiolarians, including species such as *Calocyclus turris*, *Dictyoprora armadillo*, and *Theocyrtis tuberosa*. These flanks are distinguished by sediment types such as limonites, clays, tuffs, and sandstones, which are rich in microfossils. Within the Esmeraldas Basin, particularly along the Río Cayapas, both benthic (featuring species like *Bolivina* and *Bulimina*) and planktonic foraminifera (including *Globigerina* and *Hantkenina*), as well as a variety of Late Eocene indicator radiolarians, are well-represented. This microfossil diversity underscores the paleontological richness of these areas, offering insights into the geological past of the region (Ordoñez et al., 2006).

In Pambil Fm., in a sample of gray limonite from the Río Verde, a rich association of well-preserved radiolarians was discovered, including species such as *Calocyclus* sp., *Cenosphaera* sp., and *Theocyrtis tuberosa*, suggesting a coexistence reflective of a Late Oligocene evolutionary stage. Conversely, outcrops from the Río Santiago are characterized by a broad microfauna of foraminifera and calcareous nannofossils, encompassing both

benthic and planktonic foraminifera, alongside a diversity of calcareous nannofossils and palynomorphs. These findings indicate a rich and diverse marine environment, providing invaluable insights into paleoenvironmental conditions and the evolution of marine life in these regions during the Late Oligocene (Ordoñez et al., 2006).

For the Viche Fm., in the northern section of the Río Verde Horst, atop greenish-gray and bluish claystones, a variety of microfossils were identified. The microfauna includes benthic foraminifera like *Anomalinooides incrassatus*, *Bolivina* spp., *Bulimina rostrata*, and *Uvigerina* spp.; planktonic foraminifera such as *Globigerina angustiumbilitata* and *Orbulina circularis*; calcareous nannofossils including *Coccolithus pelagicus* and *Discoaster bollii*; and a range of radiolarians like *Artostrobium miralestense* and *Calocyclus costata*, alongside palynomorphs indicative of past environmental conditions. This diverse microfossil assemblage points to a rich geological and paleoenvironmental history in the area (Ordoñez et al., 2006).

For the Angostura Fm., diverse microfauna was identified in the Santiago River outcrops, including benthic foraminifera such as *Ammonia tepida*, *Cibicidoides crebbi*, and *Uvigerina mantaensis*, along with planktonic foraminifera like *Globigerina apertura* and *Globorotalia menardii*. Calcareous nannofossils were also discovered, including *Coccolithus* sp. and *Reticulofenestra pseudoumbilica*. In the Punta Verde Horst, similar microfossils were found, with the presence of benthic foraminifera such as *Ammonia tepida* and *Amphistegina gibbosa*, as well as planktonic foraminifera including *Globigerina bulloides* and *Globorotalia acostaensis*. These findings highlight the richness and diversity of microfossil life in these areas, reflecting various marine environments and providing valuable insights into the paleoenvironmental conditions of the region (Ordoñez et al., 2006).

In the Onzole Fm., extensive and diverse microfossil communities have been identified across various locations along the west coast of Esmeraldas and in outcrops near rivers such as Santiago and Camarones, as well as in the Estero Plátano area and along the Atacames – La Unión de Atacames route. These communities, comprising both benthic and planktonic foraminifera, radiolarians, calcareous nannofossils, and palynomorphs, reflect a range of marine environments and paleoenvironmental conditions indicative of this formation (Ordoñez et al., 2006).

Within the Onzole Fm, the detection of a diverse range of benthic foraminifera ,

such as *Bolivina*, *Bulimina*, *Cassidulina*, *Cibicidoides*, and *Uvigerina*, alongside planktonic foraminifera including *Globigerina*, *Globigerinoides*, and *Globorotalia*, suggests a high level of biodiversity within the Onzole Formation. These organisms provide crucial insights into the historical salinity, temperature, and depth of the marine environment. Additionally, calcareous nannofossils, featuring species like *Coccolithus* and *Discoaster*, along with radiolarians and palynomorphs, offer further evidence of the oceanographic and climatic conditions prevailing during the formation's deposition (Ordoñez et al., 2006).

4.3 Paleoenvironment

In the Santiago Fm. the paleoenvironment is identified as a marine continental shelf. However, in the sections featuring microlumachella banks with *Discocyclusina* spp., the marine environment is characterized by depths not exceeding 50 meters, warm temperatures, and the presence of macroforaminifera, indicative of shallow, warm-water conditions (Ordoñez et al., 2006).

The Zapallo Fm. environment is characterized as warm marine waters, ranging from outer shelf to upper slope depths, indicated by the association of benthic foraminifera, the significant presence of planktonic foraminifera, and the occurrence of nassellarian radiolarians (Ordoñez et al., 2006).

For the Pambil Fm. the determined paleoenvironment was a marine setting ranging from mid to outer shelf for sediments identified in the Santiago River outcrops. This conclusion is based on the abundance and diversity of benthic foraminifera, which predominate over planktonic varieties. Additionally, a representation of continental palynomorphs, which have been transported, was found. The association of planktonic foraminifera and calcareous nannofossils suggests warm water conditions (Ordoñez et al., 2006).

For the Viche Fm. the paleoenvironment is identified as an outer shelf marine setting, deduced from the microfossil association that includes planktonic foraminifera, calcareous nannofossils, radiolarians, and some palynomorphs (Ordoñez et al., 2006).

The paleoenvironment for the Angostura Fm. is identified as an inner shelf marine setting, indicated by the occurrence of genera such as *Ammonia*, *Quinqueloculina*, *Nonionella*, and *Hanzawaia* (Ordoñez et al., 2006).

For the Onzole Fm., the sediments of the lower member are indicative of a continental shelf paleoenvironment, likely originating from the central shelf at its base, which gradually deepened towards the top. In contrast, the upper member is characterized by the abundance and diversity of benthic foraminifera, along with significant occurrences of planktonic foraminifera and calcareous nannofossils, suggesting a warm marine paleoenvironment that reaches depths up to the upper slope (Ordoñez *et al.*, 2006).

Chapter 5

Results

5.1 Seismic data improvement

One of the secondary objectives of this study was improve the quality of seismic data for geological interpretation and sequential stratigraphy, we achieved noteworthy results through the application of advanced denoising techniques, such as Noise2Void, in combination with statistical and predictive filtering methods.

The implementation of these denoising techniques has led to a remarkable improvement in the quality of the eleven lines used in this thesis, enabling the clearer visibility and differentiation of geological features. This advancement significantly aids in the interpretation of subsurface geological formations and in the application of sequential stratigraphy. By isolating and removing extraneous signals like noise, our research has facilitated a more detailed and accurate analysis of the stratigraphic layers, as it is shown in Figure 5.1, which is a zoom in to the seismic line 1A. The refined seismic data supports a more nuanced interpretation of geological structures, stratigraphic relationships, and sedimentary environments, marking a significant step forward in the field of geology and stratigraphy, offering enhanced insights into the stratigraphic evolution.

The introduction of Spectral Blueing, a technique that acts as a form of deconvolution by amplifying specific high-frequency components, has marked a significant advancement in our ability to enhance the resolution of seismic data. This enhancement allows geological layers and other subsurface features to be distinguished with greater clarity, overcoming the attenuation of high-frequency components and resulting in substantially improved image

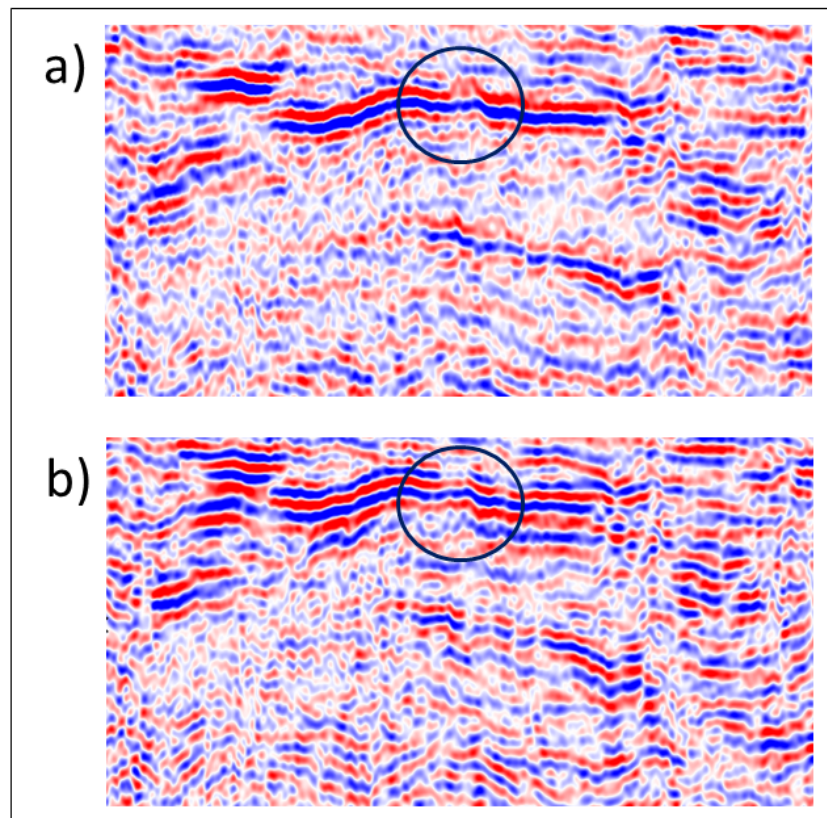


Figure 5.1: Comparison of a zoom in to the Seismic Line 1A data before and after denoising: a) Original seismic line 1A image before the denoising process, highlighting the presence of noise. b) The same seismic line 1A following the application of denoising techniques, **with a circle emphasizing a significant improvement in data clarity**, demonstrating the effectiveness of the denoising process in removing unwanted noise.

quality, as it is shown in Figure 5.2, which are different approaches to Seismic Line 10B. Our results illustrate how this technique has made geological layers more discernible, providing a deeper understanding of the subsurface geology, as can be seen in the graphs 2a, 2b and 2c of Figure 5.2 .

Furthermore, we have observed a significant increase in the correlation between seismic and well data, particularly notable in the seismic-well tie analysis conducted on the Borbón-1 well, where the correlation coefficient increased from 0.23 to 0.29, as shown in the seismic well tie of the Figure 3.5 in the column called Trace 1026b-Bourbon-1, which is the final correlation of the tie between seismic line 4A and the Borbón-1 well. This increase in correlation suggests a more precise alignment of seismic reflections with geological features identified in well data, reflecting a more accurate representation of the subsurface. The improvement in correlation highlights the effectiveness of these advanced techniques not

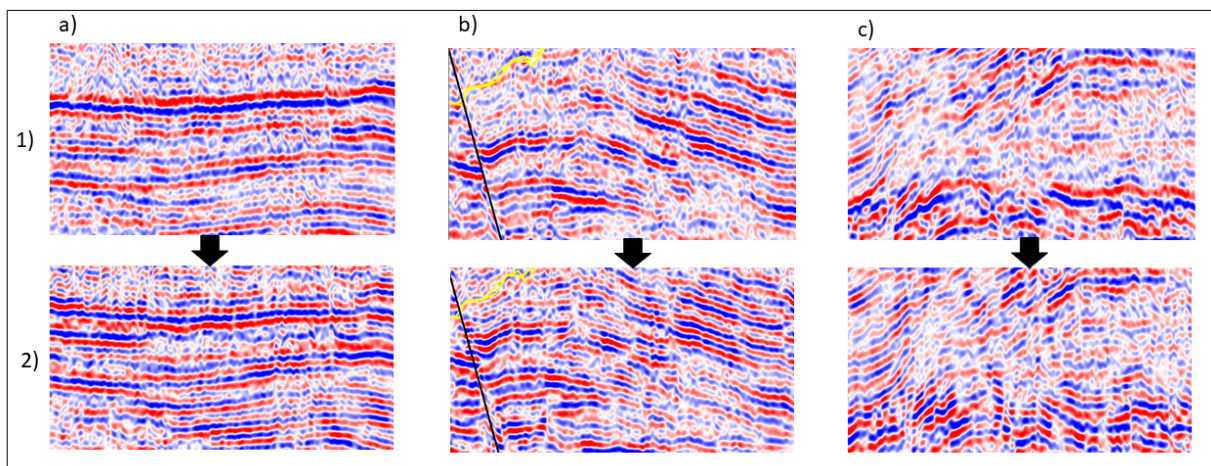


Figure 5.2: Effects of Spectral Blueing on of a zoom in to the Seismic Line 10B: The images display seismic lines before (in the row 1) and after (in the row 2) the application of Spectral Blueing. In images a) and c), Spectral Blueing accentuates specific frequencies, aiming to enhance seismic resolution. While, image b) demonstrates enhanced continuity of seismic lines, making a fault (marked with a yellow line) more visibly distinct.

only in enhancing the clarity and resolution of seismic data but also in their ability to improve data integration and confidence in geological interpretation.

5.2 Sequence stratigraphy

The exploration of the area's sequential stratigraphy has been markedly enhanced by combining seismic line analysis, geological horizons, and well logs, with bibliographic evidence, leading to the identification of the basement and five seismic stratigraphic sequences, labeled from A to E, called, from the earliest to the latest: (A) Santiago, Zapallo, Punta Ostiones, (B) Pambil, (C) Viche, (D) Lower Onzole, Angostura and (E) Upper Onzole, Cachabí, also defined in different separate investigations (Evans and Whittaker, 1982; Jaillard et al., 1997; Deniaud, 2000). These stratigraphic sequences have been rigorously defined by their unique unconformities, serving as key indicators of geological epochs and processes. In this case study of the Borbón Esmeraldas basin the recognition and detailed examination of these sequences, marked by unconformities Ub, U1, U2, U3, and U4, are crucial for comprehending the sedimentary architecture and the basin's geological evolution. These regional unconformities function as critical demarcations between the stratigraphic sequences.

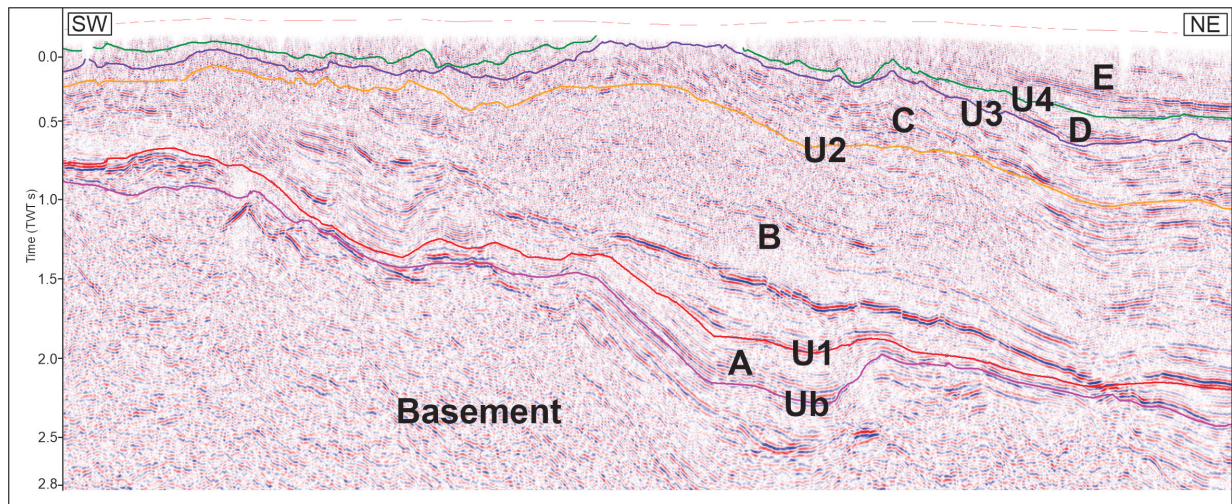


Figure 5.3: Seismic line 3A: showing the representative reflectors within each sequence (A to E) to illustrate their geometry, along with the unconformities Ub, U1, U2, U3, U4. To see the location of the seismic line consult the Figure 1.1.

The stratigraphic sequences within the Borbón-Esmeraldas basin, when correlated to their geological ages, elucidate the temporal and stratigraphic development of the area. The sequences are identified as follows: Sequence A extends from the Middle to Late Eocene, Sequence B spans from the Middle to Late Oligocene, Sequence C ranges from the Early Miocene to Late Miocene, Sequence D is dated to the Late Miocene, and finally, Sequence E encompasses the period from the Pliocene to Pleistocene. This organization provides a structured timeline, illustrating the evolution of the basin from the Late Cretaceous through to the Pleistocene.

5.2.1 Major unconformities

The elucidation of the area's stratigraphy through the integration of seismic analyses, geological horizons, and well log data, has significantly advanced our understanding of the sequential development of the basin. This comprehensive approach has facilitated the delineation of four distinct seismic stratigraphic sequences in the Esmeraldas-Borbón Basin. In this case study of the Borbón Esmeraldas basin, these sequences are demarcated by the unconformities Ub, U1, U2, U3, and U4 (Figure 5.4). The earliest unconformity, labelled Ub, is associated to a sedimentary hiatus related to a pre-Eocene erosion, also defined by [Jaillard et al. \(1997\)](#), and the later unconformities, labelled from U1 to U4, are dated U1: 36–34, U2: 24–22, U3: 14–12, and U4: 5 Ma, respectively, based on the

dating of the ages of the formations according to (Evans and Whittaker, 1982; Jaillard et al., 1997; Deniaud, 2000). The presence of these regional unconformities, which act as critical junctures between this stratigraphic sequences from A to E, highlights the dynamic processes of sediment deposition and erosion, offering insights into the geological forces at play over time.

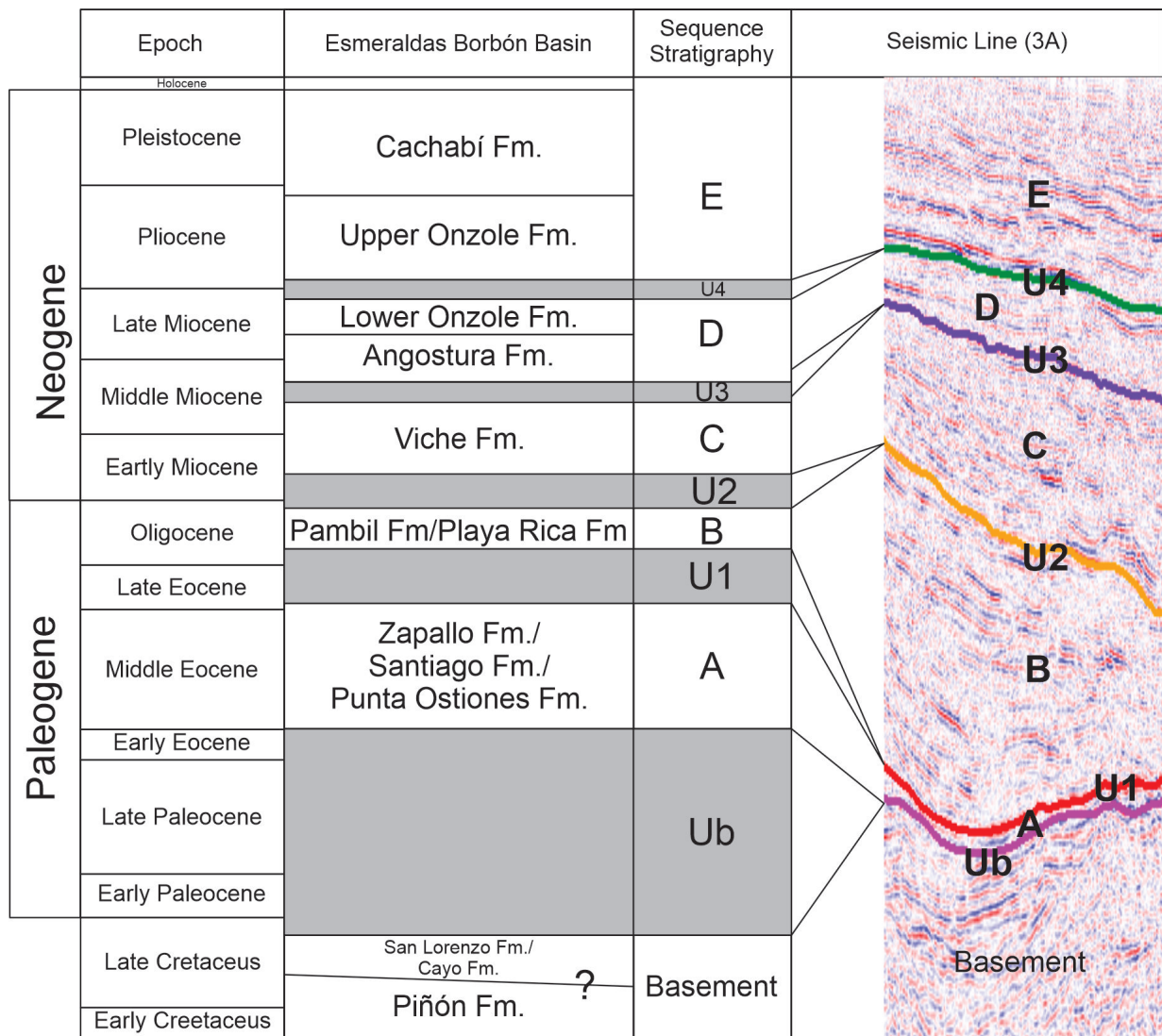


Figure 5.4: Correlation between seismic units A to E of the Esmeraldas Borbón Basin and the unconformities Ub to U4 in relation to the geological formations. This visualization includes a detailed focus on seismic line 3A, highlighting the key features and the interaction between the seismic units and the geological formations. The Esmeraldas Borbón basins is based on: Pre-Oligocene chronostratigraphy is from (Jaillard et al., 1997); the Neogene chronostratigraphy is from (Deniaud, 2000; Marcaillou and Collot, 2008; Reyes and Michaud, 2012)

The stratigraphic framework within the Borbón-Esmeraldas basin is defined by sig-

nificant unconformities spanning from the Late Cretaceous to the Pliocene, as illustrated in Figure 5.4. Unconformity Ub marks a critical boundary from the Late Cretaceous to the Early Eocene, delineating the transition between early Eocene sedimentary units and the underlying basement, indicating a shift in depositional environments. U1, from the Upper Late Eocene to the Middle Oligocene, acts as a Sequence Boundary (SB) Type 2, represented by Transgression and Regression. U2, located in the early Early Miocene is identified as Sequence Boundary Type 1, highlighting a phase regression and transgression. U3 transitions from an Transgression to regression at the end of the Middle Miocene and is categorized as Sequence Boundary Type 2. U4, extending from the Late Miocene to the Pliocene indicating widespread marine deposits before transgression, and is identified as Sequence Boundary Type 1, as depicted in Figure 5.4. These unconformities underscore the basin's complex geological evolution, influenced by sedimentation and tectonic activities, showcasing the intricate relationship between geological events and sedimentary processes. This detailed understanding facilitates insights into past environmental conditions, providing a comprehensive picture of the basin's development over geological time.

5.2.2 Basement

Seismic reflection data provide insights into the basement's geological composition, indicating a low amplitude, chaotic, and discontinuous seismic reflections (Figure 1) typically associated with the high lithification and uniform acoustic properties of the igneous and metamorphic rocks constituting this layer. Situated at depths exceeding 3100 meters (Figure 5.5), the basement presents a massive chaotic structure that spans the entire basin, laying a profound foundation beneath the overlying sedimentary sequences.

The basement, defined at its upper boundary by the Ub unconformity and ranging from the Cretaceous to the Late Cretaceous, encompasses the Piñon Formation, which constitutes the foundation across Ecuadorian coastal basins. Comprising primarily extrusive volcanic rocks, the Piñon Formation is characterized by diabases, pillow lavas, and theolitic basalts, reflecting a complex volcanic origin.

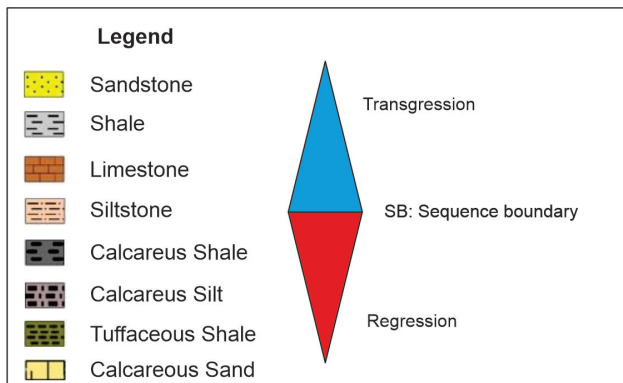
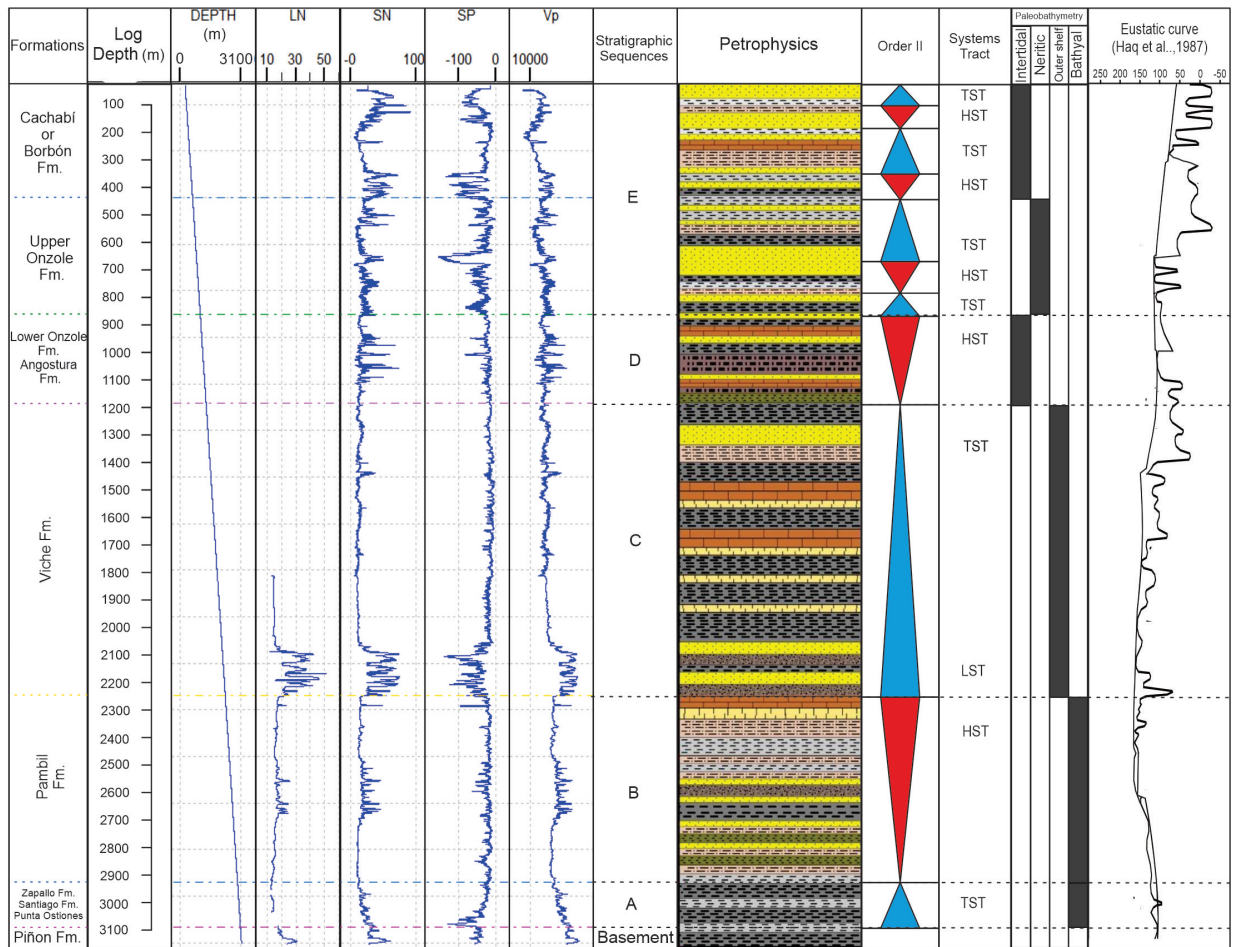


Figure 5.5: Schematic Sequential Stratigraphy of the Borbón-Esmeraldas Basin: This illustration encapsulates comprehensive log data from Borbón-1, including Lithium Neutron (LN) logs in porosity (percentage), Sonic Neutron (SN) logs in microseconds per foot (us/ft), Spontaneous Potential (SP) in millivolts (mV), and P-wave Velocity (Vp) in feet per second (ft/s). The figure meticulously outlines the corresponding lithologies for each formation, sequences from A to E, identifies unconformities and boundaries with second-order, transgressive-regressive (T-R) cycles, paleobathymetry, and integrates the Eustatic curve following [Haq et al., 1987], providing a detailed view of the basin’s stratigraphic dynamics.

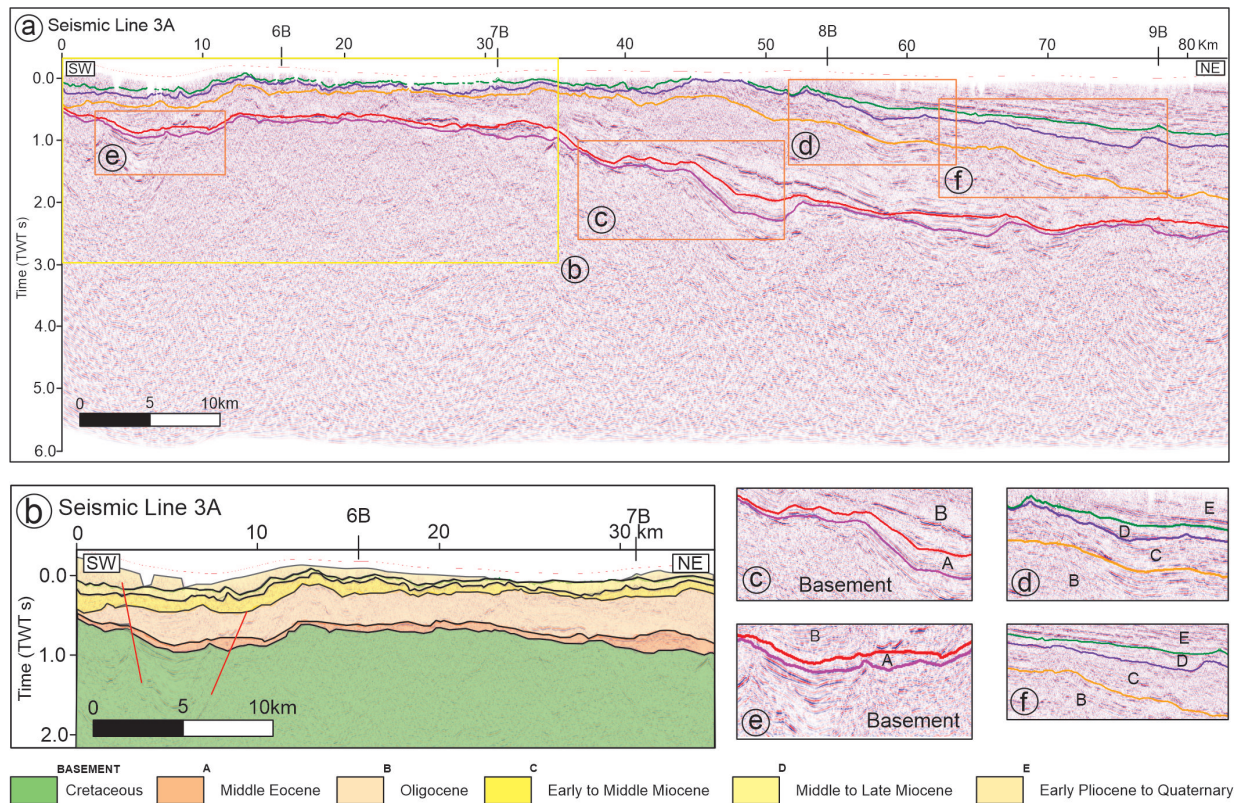


Figure 5.6: a) Seismic Line A3 (location in Figure 1.1); b) a segment of Seismic Line A3 selected for constructing stratigraphic sequences, highlighting representative reflectors within each sequence to illustrate their geometry—the (location of this segment is marked by a yellow box); c), d), e), and f) present detailed views of the seismic profile from Seismic Line 3A (detailed section is identified by orange boxes).

5.2.3 Sequence stratigraphy A (Middle to Late Eocene)

The Sequence Stratigraphy A, from the Middle to Late Eocene (Figure 1b), is characterized by the basal unconformity U_b , marking its lower boundary and differentiating it from the underlying Piñon Formation basement in the Borbón-Esmeraldas basin (Figures 1c, and 1e). This significant geological transition heralds the start of sedimentary deposition. Thickness varies significantly across locations, with about 210 meters recorded in the Borbón-1 well between depths of 2,900 to 3,000 meters (Figure 5.5), 200 meters in the Telembí-1 well from 1,200 to 1,400 meters, and in certain areas extending up to 610 meters, illustrating the sequence's spatial variability within the basin.

Encompassing the Santiago, Punta Ostiones, and Zapallo Formations, the sequence underscores a period of dynamic sedimentary processes and environmental shifts. This sequence is primarily composed of forearc sediments, starting with a discontinuous limestone

unit at its base, followed upwards by shales with carbonate intervals and calcareous sandstones (Figure 5.5). It reflects a marine paleoenvironment associated with the continental shelf, likely extending from the outer shelf to the upper slope, primarily constituting a carbonate facies.

The Isopach Map 5.7 delineates sediment distribution within the study area, highlighting the northeast's thickest deposits in blue, indicating a depocenter. This may result from sediment sourcing from the northeast or favorable subsidence patterns. Conversely, sediment thickness diminishes towards the southwest, shown in green, reflecting a decrease in sediment supply or changes in depositional conditions. The northwest and southeast display very low sediment thickness, suggesting minimal deposition likely due to elevated topography or remoteness from the sediment source.

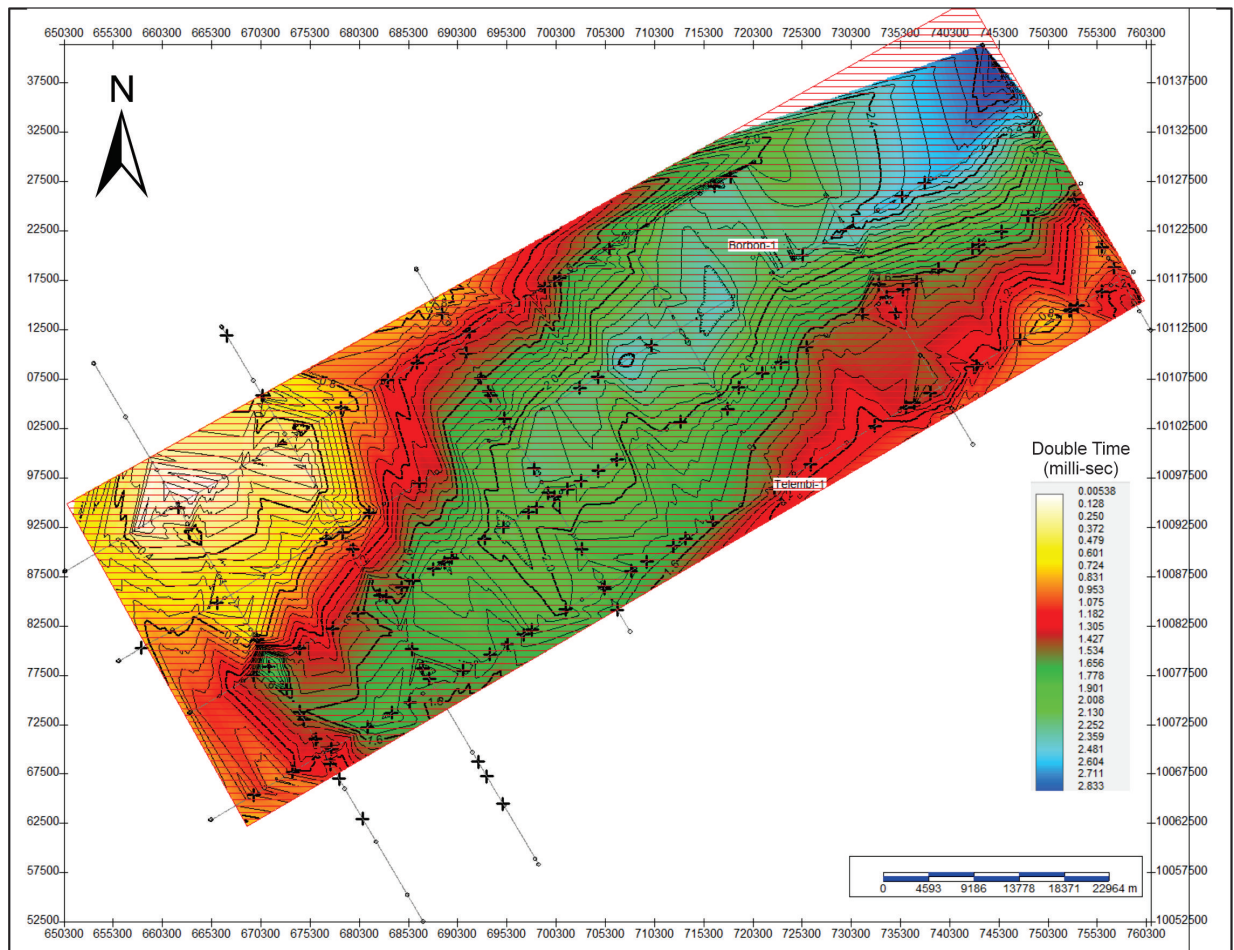


Figure 5.7: Isopach Map of Sequence Stratigraphy A (Middle to Late Eocene): This map showcases the distribution of sediment thickness across the region, where sediment accumulation is maximized (depocenter), are clearly delineated alongside structural highs.

5.2.4 Sequence stratigraphy B (Middle Oligocene to Late Oligocene)

Sequence B, spanning the Middle to Late Oligocene (Figure 1b), is delineated at its base by the U1 unconformity. Its seismic reflection character is dominated by low to medium amplitude, wavy to chaotic, and discontinuous reflections (wavy seismic facie) (Figures 1c, 1d, 1e, and 1f). Within the Borbón-1 well, Sequence B shows a thickness of 400 meters across depth intervals from 2,900 to 2,500 meters (Figure 5.5). Similarly, in the Telembí-1 well, it also reaches a thickness of 400 meters, but from 1,200 to 800 meters in depth. This uniformity in thickness and the mirrored structural relief distribution across the study area highlight a consistent geological framework for Sequence B.

Primarily including the Pambil and Playa Rica Formations, this sequence is lithologically composed of claystone and fine-grained sandstone (Figure 5.5). Its biostratigraphy is characterized by a rich fossil fauna, including brachiopods, bryozoans, echinoderms, mollusks, and planktonic foraminifera, pointing to a marine setting. This description corresponds to a Siliciclastic Facies, specifically suggesting a marine environment.

The sediment distribution the Sequence B shown in the Isopach Map 5.8, with its depocenter in the northeast, indicates that this region is the primary sediment source, tapering towards the west. This pattern, coupled with a shallowing-upward trend and the presence of warm-water microfossils, suggests a prograding shoreline advancing into deeper marine settings. This environment, shaped by marine is marked by dynamic, warm, shallow marine conditions, highlighting a complex interplay between sediment sources, transport, and environmental factors. The isopach map underscores the formation's geological framework, evidencing sedimentation patterns and environmental shifts.

5.2.5 Sequence stratigraphy C (Early Miocene to Middle Miocene)

Sequence C, defined at its lower boundary by the U2 unconformity and spanning from the Early Miocene to the Middle Miocene (Figure 1b), is characterized by seismic reflectors displaying oblique to parallel reflections that are continuous and semicontinuous with low-to-high amplitudes (Figures 1d, and 1f). Within the Borbón-1 well, this sequence shows a thickness of approximately 200 meters, covering depth intervals from 2,500 to 2,300 meters

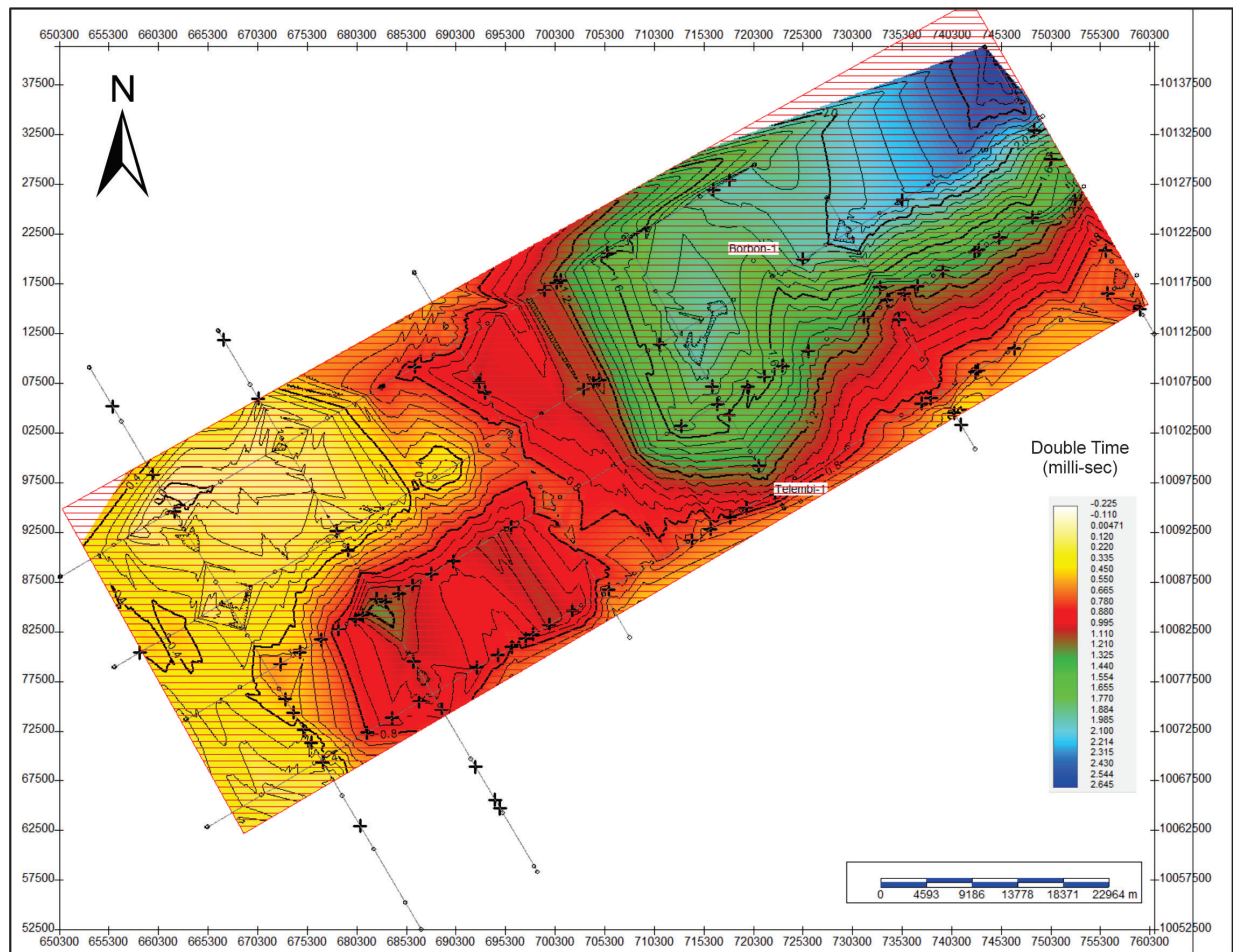


Figure 5.8: Isopach Map of Sequence stratigraphy B (Middle Oligocene to Late Oligocene): This map showcases the distribution of sediment thickness across the region, where sediment accumulation is maximized (depocenter), are clearly delineated alongside structural highs.

(Figure 5.5). However, the narrative mistakenly mentions Sequence D in the Telembi-1 well, which should be corrected to Sequence C, reflecting significant sedimentary accumulation within these intervals and across the study area, with combined thicknesses potentially reaching up to 600 meters.

This sequence primarily includes the Viche Formation. Characterized by claystone with interbedded fine-grained sandstone (Figure 5.5), which are locally rich in mollusks and fish scales, the Viche Formation indicates an outer shelf marine environment.

The isopach map 5.9 of the Sequence C displays a pattern of very low sediment accumulation in the south and southwest, highlighted by widespread yellow areas indicating reduced deposition. This uniform thinness across the formation suggests a consistent,

shallow depositional environment, likely affected by uniform sediment supply and tectonic influences. The transition from proximal to distal depositional settings, suggested by the sediment distribution and the map's discordance show points to the impact of tectonic activities and the westward progradation of the coastline. Microfossil evidence supports a outer shelf marine environment, highlighting the complex interplay of geological forces that shaped the sedimentation patterns observed.

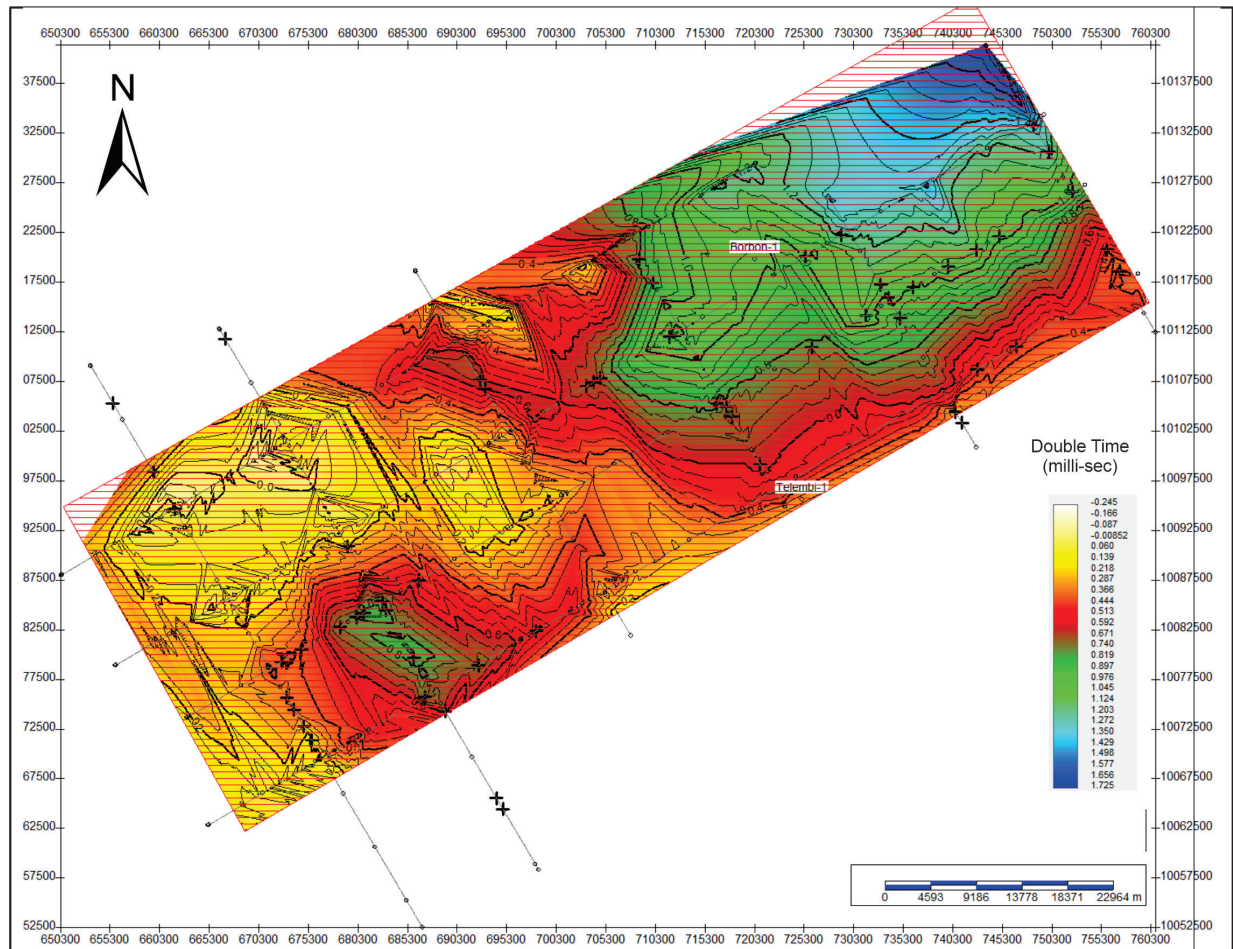


Figure 5.9: Sequence stratigraphy C (Early Miocene to Middle Miocene): This map shows the distribution of sediment thickness across the region, where sediment accumulation is maximized (depocenter), are clearly delineated alongside structural highs.

5.2.6 Sequence stratigraphy D (Late Miocene)

The stratigraphic Sequence D, identified by the U3 unconformity at its base, covers the Late Miocene (Figure 1b) period and is marked by seismic reflections ranging from oblique to parallel, which are continuous to semicontinuous with varying amplitudes from low to

high (Figures 1d, and 1f). This sequence is prominently featured within the Borbón-1 well, where it exhibits a significant thickness of 1,000 meters across depth intervals from 2,300 to 1,300 meters (Figure 5.5). Sequence E, succeeding Sequence D, is absent in the Telembí-1 well, highlighting the uneven distribution of these sequences across various regions within the basin. Such variability emphasizes the complex deposition patterns and stratigraphic diversity that define the Late Miocene period.

This sequence encompasses the Angostura and Lower Onzole Formations, characterized by a base of sandstone and siltstone. Progressing upwards, it transitions into layers of siltstone and conglomeratic claststone, culminating in the highest portion with argillaceous siltstone interbedded with sandstone (Figure 5.5). This stratigraphic sequence indicates a Siliciclastic Marine Facies that reflects a range of depositional processes occurring in an open marine inner shelf environment.

The sediment distribution in Sequence D illustrates depositional dynamics and environmental shifts, with high sediment thickness in the northwest, indicating significant accumulation due to proximity to sediment sources, subsidence, or preservation-friendly conditions. Moving eastward, sediment accumulation decreases, suggesting reduced supply or increased energy affecting deposition. The southwest, with the lowest sediment thickness, points to areas further from sources or under higher energy conditions limiting deposition. This gradation suggests a transition from deeper marine to shallower platform environments, likely reflecting a prograding coastline or deltaic system. The isopach map reveals a pattern shaped by sediment supply, depositional energy with the northwest as the primary depocenter, as shown in Figure 5.10.

5.2.7 Sequence stratigraphy E (Oligocene to Pleistocene)

Sequence E, defined by the U4 unconformity at its base, extends from the Pliocene through to the Pleistocene (Figure 1b). Seismic lines reveal reflections that range from oblique to parallel, continuous in nature, with amplitudes from low to high (Figures 1d, and 1f). Within the Borbón-1 well, this sequence demonstrates a notable thickness of 300 meters, covering depth intervals from 1,300 to 1,000 meters (Figure 5.5), highlighting its substantial geological presence during this time period.

Incorporating the Cachabí, Borbón, and Súa Formations, this stratigraphic sequence

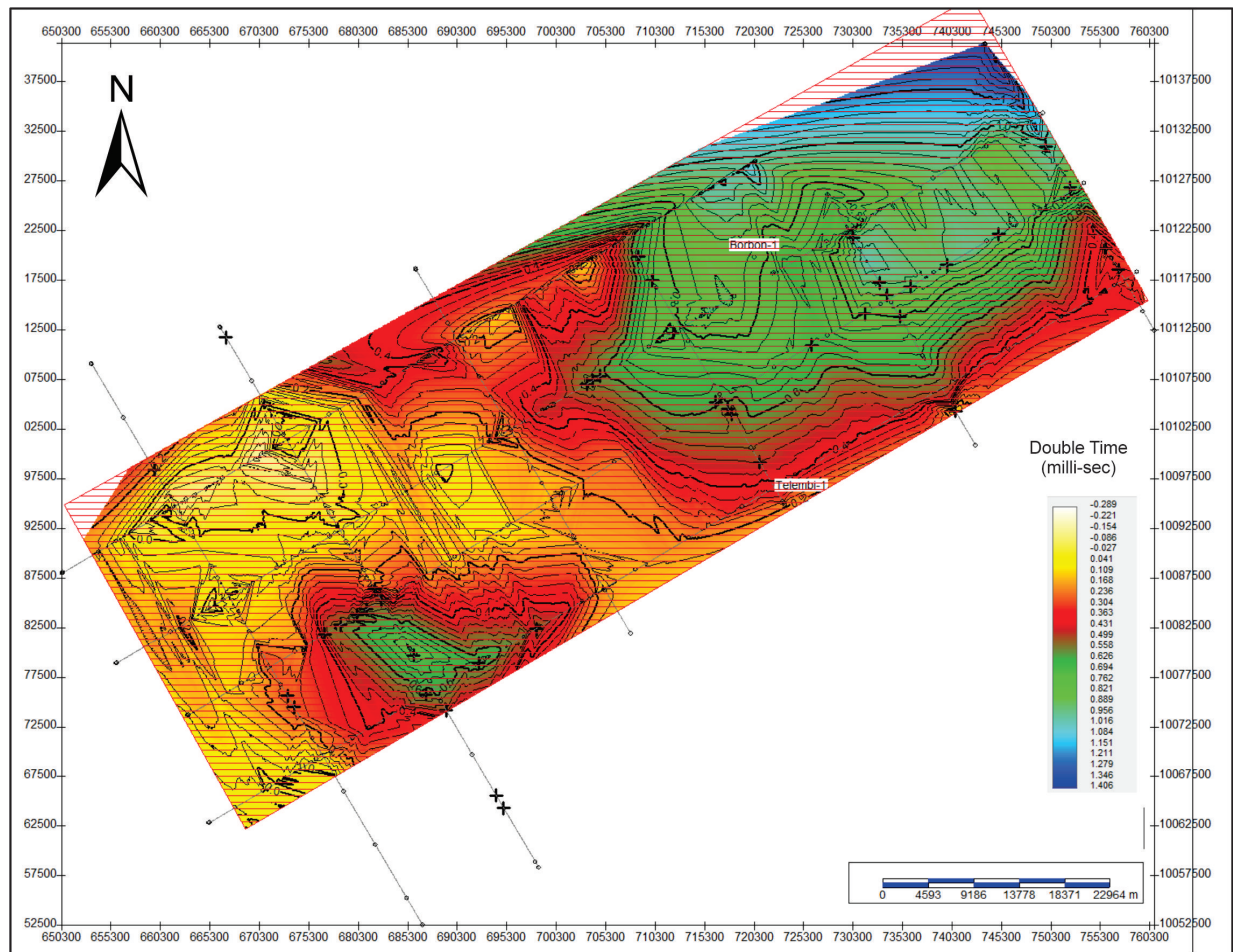


Figure 5.10: Sequence stratigraphy D (Late Miocene): This map showcases the distribution of sediment thickness across the region, where sediment accumulation is maximized (depocenter), are clearly delineated alongside structural highs.

showcases a base of sandstone and conglomerate, followed by layers of interbedded claystone and siltstone, with the uppermost section, belonging to the Borbón Formation, predominantly consisting of sandstone (Figure 5.5). The depositional history of this formation reveals a regressive transition from a shallow marine to a transitional environment, subsequently followed by a transgressive phase characterized by the emergence of shell beds in the upper section, culminating in a regional uplift. This progression reflects a dynamic geological history, encapsulating shifts in environmental conditions over time.

5.3 Subsidence analysis

The subsidence analysis conducted through the interpretation of geohistorical graphs provides a crucial understanding of the temporal and spatial variations in basin development. These analyses are instrumental in reconstructing the subsidence history of a basin, offering insights into the processes governing its evolution. By examining the patterns and rates of subsidence over geological time, we can infer the tectonic activities, sediment accumulation rates, and environmental conditions that have influenced the basin's formation and modification. Geohistorical graphs serve as a window into the past, allowing us to visualize changes in subsidence through time and relate these changes to broader geological events such as orogeny, rifting, and eustatic sea-level fluctuations.

The data for the geohistorical graph analysis of the Borbón-Esmeraldas basin are derived from a variety of sources, with sediment thickness, age, and lithology obtained from well logs and literature. Initial porosity, compaction constants, and sediment density values are sourced from the standard parameters outlined by Gallagher and Lambeck (1989). Paleobathymetry estimates are based on facies analysis, providing insight into historical water depths and sedimentary environments. Sea-level variations are inferred from the global sea-level change curve proposed by Haq et al. (1987), offering a framework to interpret the basin's depositional history in the context of global eustatic sea-level fluctuations. This comprehensive approach integrates diverse data sets to reconstruct the basin's development and understand the interplay between local sedimentary processes and global geological events.

For this thesis, subsidence analysis was conducted exclusively on the Borbón-1 and Telembí-1 well logs, with Borbón-1 being the only complete dataset. For each well, the evolution of subsidence and tectonic activity was calculated, and the results are depicted in the respective geohistorical graphs. This focused approach allows for a detailed examination of subsidence patterns and tectonic influences within these specific locations, contributing to a deeper understanding of the basin's geological development.

5.3.1 Borbón-1

The subsidence analysis from the Borbón-1 well log reveals a layered narrative of the Borbón-Esmeraldas basin's geological development, characterized by distinct phases of sedimentary deposition correlated with significant geological epochs. Initially Sequence A, capturing the Santiago and Zapallo Formations from 41 to 38 Ma, marks the onset of geological deposition. This is followed by Sequence B, with the Pambil and Playa Rica Formations from 33 to 23 Ma, indicating a period of intensified subsidence. Sequence C, associated with the Viche Formation from 20 to 14 Ma, represents the most pronounced subsidence phase, suggesting a rapid sedimentary accumulation. Subsequently, Sequence D spans from 12 to 7.4 Ma, covering the Angostura and Lower Onzole Formations. Lastly, Sequence E, from 5 to 0.0117 Ma, involves the Borbón Formation and Súa Member, showing a decrease in subsidence intensity. These sequences are separated by unconformities U1, U2, U3, and U4, each marking a gap of 3 to 5 Ma, indicating significant geological transitions, as shown in Figure 5.11.

The subsidence patterns elucidated by the Borbón-1 well log offer profound insights into the basin's sedimentary and tectonic dynamics. The correlation between subsidence events and geological formations provides evidence of the interplay between tectonic forces, sediment supply, and sea-level fluctuations over millions of years. The pronounced subsidence observed in Sequence C, for instance, may indicate accelerated tectonic activity or a significant sea-level fall, leading to a rapid increase in sediment accommodation space, in terms of the slope it would be an increasing subsidence. Besides, the subsidence that appears in sequence A is the initial subsidence that formed the basin, and after this, several sequences of decreasing subsidence were formed, which are what formed the stratigraphic sequences B, D, and E. Meanwhile, the gaps identified by the unconformities signify periods of substantial environmental or tectonic changes, serving as crucial markers for understanding the basin's paleoenvironmental history. The analysis unveils that all unconformities are associated with negative subsidence rates, indicative of erosional periods or non-depositional phases that punctuate the geological record, which would be related to an exhumation phenomenon. These negative values suggest episodes where the basin experienced uplift or a decrease in accommodation space, leading to erosion or the halting of sediment deposition.

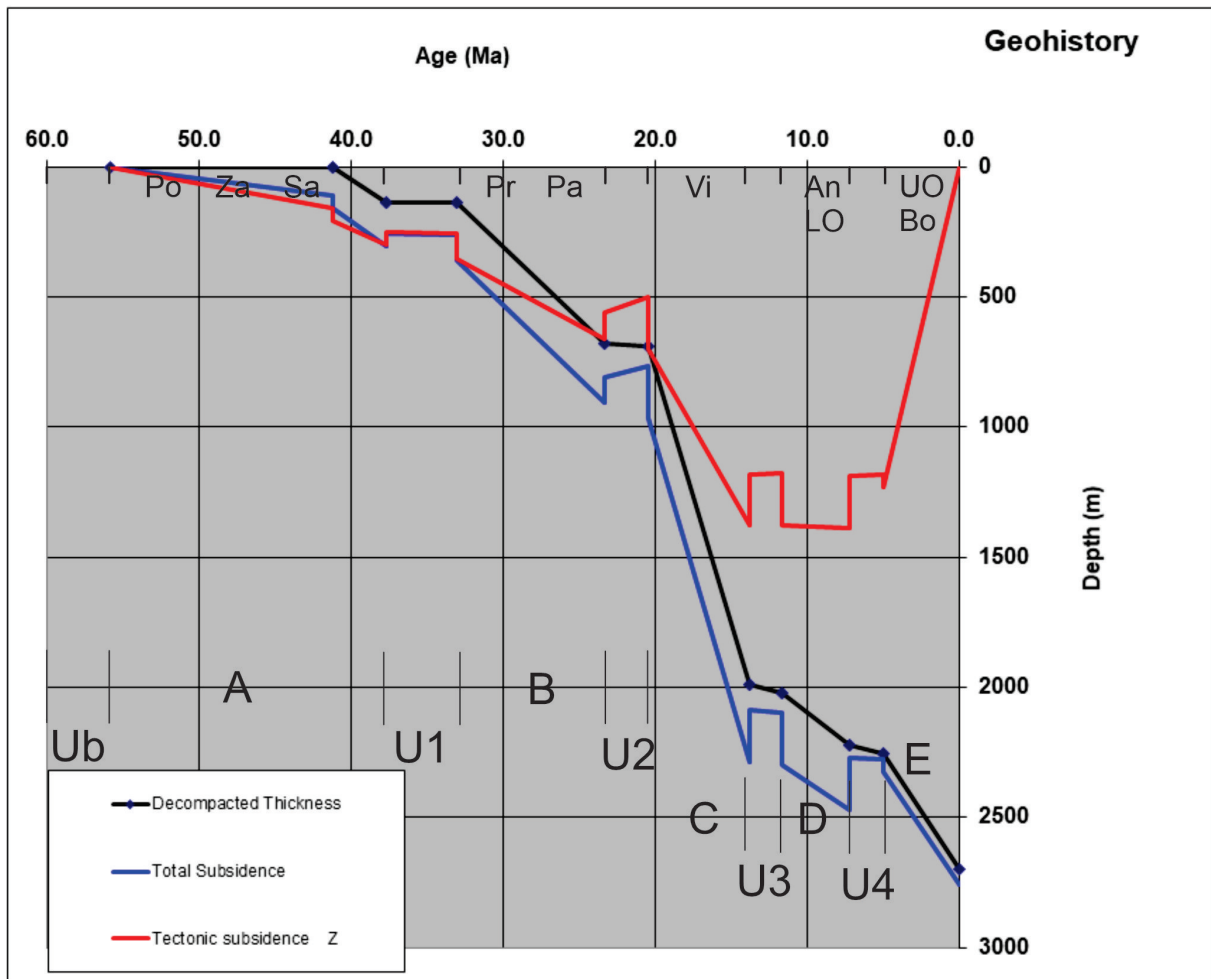


Figure 5.11: Geohistorical Chart of Borbón-1 Well: This chart provides a detailed view of the chronological development and sedimentary sequences within the Borbón-1 well, illustrating Sequences A, B, C, D, and E. It also marks the key unconformities U1, U2, U3, and U4.

This comprehensive analysis of subsidence patterns not only enhances our understanding of the Borbón-Esmeraldas basin’s geological evolution but also contributes valuable insights into the complex processes influencing sedimentary basin development on a broader scale.

5.3.2 Telembí-1

The Telembí-1 well log subsidence analysis provides a detailed stratigraphic overview of the Telembí area within the Borbón-Esmeraldas basin, identifying four main sedimentary sequences: A, B, D, and E. These sequences reflect the basin’s sedimentary infill and tectonic adjustments from the early Eocene to the Pleistocene. Initial sedimentation,

Sequence A, spans from 41 to 38 Ma, documenting the earliest phase of deposition. This is followed by Sequence B (33 to 23 Ma) and Sequence D (20 to 14 Ma), each marking progressive stages of sediment accumulation and basin development. Notably, Sequence E, extending from 5 to 0.0117 Ma, captures the latest depositional phase. Unconformities U1, U2, and U4 delineate these sequences, with each representing significant geological shifts. The absence of Sequence D and the extended duration of unconformity U4 underscore a prolonged phase of geological stability or non-deposition, reflecting a distinct evolutionary path compared to the Borbón-1 analysis, as shown in Figure 5.12.

In the Telembí-1 well, the extended duration of the U3 unconformity highlights a period of pronounced geological inactivity or erosional processes, differentiating it from the Borbón-1 well's sequence. This extended gap suggests a more significant impact of tectonic uplift or environmental changes, leading to a prolonged interruption in sedimentation. Such disparities in subsidence patterns and unconformity durations between the Telembí-1 and Borbón-1 wells emphasize the complexity of the basin's development, showing that the further east of the Borbón Esmeraldas basin the moments of exhumation were higher or lasted longer in exhumation than the west of the Basin.

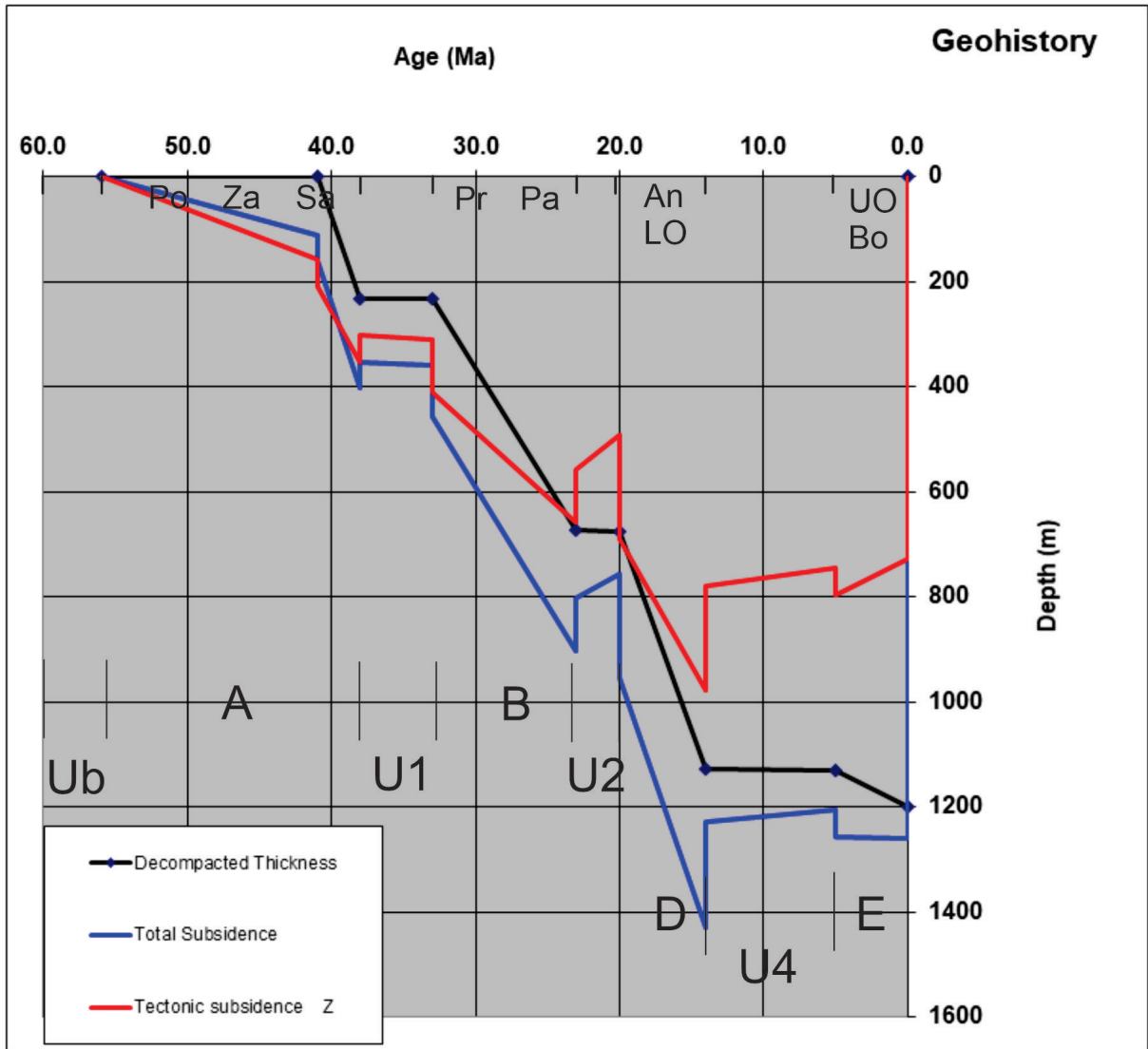


Figure 5.12: Geohistorical Chart of Telembí-1 Well: This chart provides a detailed view of the chronological development and sedimentary sequences within the Borbón-1 well, illustrating Sequences A, B, D, and E. It also marks the key unconformities U1, U2, and U4.

Chapter 6

Discussion

6.1 Sedimentation and Tectonic history of the Esmeraldas Borbón Basin

The knowledge presented from the sequences and geohistory discussed above allows us to identify a minimum of five tectonic episodes that have governed the sedimentary development of the Esmeraldas-Bourbon basins from the Late Cretaceous to the present. Understanding these events is critical to understanding tectonic impacts in the Esmeraldas Borbón Basin, as this understanding is reinforced by both previous research and the data presented in this discussion.

6.1.1 First tectonic phase: Latest Cretaceous–Paleocene

The late Eocene-early Oligocene tectonic phase is widely acknowledged throughout the Andes as the Incaic phase, as identified by [Mégard \(1984\)](#). This period has been linked to a regional plate kinematic shift, as evidenced by [Jaillard and Soler \(1996\)](#); [Noblet et al. \(1996\)](#). Consequently, we propose that U1 correlates with this significant regional tectonic phase. The oceanic basement of the Esmeraldas Borbón Basin was accreted prior to the deposition of Unit A, during either the Paleocene or the Late Cretaceous, confirmed with findings reported by [Jaillard et al. \(1997\)](#); [Luzieux \(2007\)](#); [Lebrat et al. \(1987\)](#). Therefore, this tectonic phase was instrumental in the erosion of the Ub surface and in the deformation within the Basement.

6.1.2 Second tectonic phase: Late Eocene–Early Oligocene

In the Esmeraldas Borbón Basin, event U1 happened before Unit B was laid down, likely at the time when the Eocene period changed to the Oligocene. This timing matches with very high rates of rock uplift dated between 43 and 30 Ma in the Cordillera Real of Ecuador, as reported by [Spikings et al. \(2001b\)](#). According to what [Jaillard and Soler \(1996\)](#), this significant geological event might have been caused by changes in the way the Earth's plates moved. It is likely linked to the Inca tectonic phase, which happened around 40 to 35 Ma, as [Mégard \(1984\)](#). This tectonic phase is also believed to have played a key role in creating the main area where sediments accumulated in the basin, shown in Figure 5.7.

6.1.3 Third tectonic phase: Late Oligocene–Early Miocene

Deposition of Unit D commenced in the Late Oligocene across all basins shaped by earlier phases of deformation. The third deformation phase, marked by compression, is evidenced by the folding observed in Seismic Sequence B. This compressive phase started after Unit B was deposited and peaked in the late Oligocene-early Miocene period, coinciding with the widespread U2 unconformity, which might have been an erosion surface at the crest of the uplift. Identified across the region [Jaillard et al. \(1997\)](#), this phase was likely driven by the splitting of the Farallon Plate around 23 million years ago (Ma), as noted by [Lonsdale \(2005\)](#).

6.1.4 Fourth tectonic phase: Middle Miocene

During the early to middle part of the Miocene epoch, the main events happening along the edge were the subsidence and the sedimentation of layers of earth or other materials. This is evident from the widespread presence of Unit C (Figure 1). Moving into the middle Miocene, the area again underwent compressive forces, leading to the creation of U3 (Figure 5.4). This time of compression in the middle Miocene is especially noticeable along the coastlines of Ecuador and Colombia. It coincides with a time when the mountains in Ecuador's Cordillera Real were being very actively uplifted, around 15 million years ago, as reported by [Spikings et al. \(2001b\)](#). This led to the erosion of land and might have caused parts of the Esmeraldas Borbón basin to be exposed or uplifted, a process referred

to as exhumation.

6.1.5 Fifth tectonic phase: Early Pliocene to Present

Following the intense compressive period in the middle Miocene, the geological dynamics of the Esmeraldas Borbón Basin changed significantly. This part of the margin went through a phase of subsidence, and the accumulation of sediment from the late Miocene to the Pliocene era. Around 5 million years ago, this subsidence process in the Esmeraldas Borbón Basin was halted, leading to the formation of the U1 unconformity. Then, the depositing of sediment and the sinking resumed during the Plio-Quaternary, as evidenced by the sediment layers of Unit E. After this pause, the process of depositing sediments from land into the ocean continued, contributing further to the development of Unit E.

Chapter 7

Conclusions

- This research markedly improved the quality of seismic data for geological analysis through the application of sophisticated denoising methods, including Noise2Void, and statistical filtering techniques. These approaches successfully minimized both random and coherent noise, leading to enhanced seismic imagery. Such advancements enabled more precise identification of geological features, thereby supporting in-depth subsurface examination and the delineation of stratigraphic sequences. The analysis of the Borbón-1 well demonstrated a significant enhancement in the correlation ($c=29$) between seismic and well data, underscoring the effectiveness of improving data coherence.
- Through the integration of seismic analysis, geological horizons, and well log data, our study has significantly deepened the understanding of the Esmeraldas-Borbón Basin's sequential stratigraphy, identifying five distinct seismic stratigraphic sequences marked by critical unconformities. These sequences and their bounding unconformities—Ub, U1, U2, U3, and U4—provide a window into the complex sedimentary architecture and evolutionary history of the basin, from the Late Cretaceous through the Pliocene. Each unconformity, serving as a pivotal geological marker, reflects the dynamic interplay of sedimentation and erosion processes, shaped by fluctuating sea levels and tectonic activities.
- The detailed analysis of sediment distribution, particularly through isopach mapping, underscores regional depositional trends and environmental shifts, providing insights

into the basin's complex depositional history and stratigraphic variability. This work not only enhances our understanding of the basin's geological evolution but also contributes to the broader knowledge of sedimentary basin development over geological time.

- Through comprehensive subsidence analysis utilizing geohistorical graphs, this study offers a deep dive into the temporal and spatial development of the Borbón-Esmeraldas basin. The focused analyses on the Borbón-1 and Telembí-1 wells reveal distinct phases of subsidence, each marked by unique sedimentary sequences and punctuated by periods of erosion or non-deposition, highlighted by the unconformities.
- The sedimentation and tectonic history of the Esmeraldas Borbón Basin reveals a complex evolution shaped by at least five significant tectonic episodes from the Late Cretaceous to the present. The identification of these phases, including the Incaic phase and others marked by major shifts in plate kinematics, regional uplift, and sediment deposition, has been crucial in understanding the geological development of the basin. The initial phase involved the accretion of the oceanic basement and was followed by periods of uplift, compression, and sedimentation that led to the formation of various geological units. This series of tectonic events not only crafted the current landscape but also influenced the deposition patterns and the erosion processes within the basin.

Bibliography

- Aizprua, C., Witt, C., Johansen, S. E., and Barba, D. (2019). Cenozoic stages of forearc evolution following the accretion of a sliver from the late cretaceous-caribbean large igneous province: Sw ecuador-nw peru. *Tectonics*, 38:1441–1465.
- Allen, P. A. and Allen, J. R. (2013). *Basin analysis: Principles and application to petroleum play assessment*. John Wiley & Sons.
- Benitez, S. (1995). Évolution géodynamique de la province côtière sud-équatorienne au crétacé supérieur-tertiaire.
- Birnie, C., Ravasi, M., Liu, S., and Alkhalifah, T. (2021). The potential of self-supervised networks for random noise suppression in seismic data. *Artificial Intelligence in Geosciences*, 2:47–59.
- Bristow, C. and Hoffstetter, R. (1977). *Léxico Estratigráfico del Ecuador*.
- Bueno Salazar, R. (1989). Hydrocarbon exploration and potential of the pacific coastal basin of colombia. In Ericksen, G., Canas Pinochet, M., and Reinemund, J., editors, *Geology of the Andes and its relation to hydrocarbon and mineral resources*, Circum-Pacific Council for Energy and Mineral Resources Earth Sciences Series, pages 335–343, Houston, Texas.
- Carrillo, E., Barragán, R., Vázquez-Taset, Y., Almeida, R., Chalampunte, A., and Martín, G. (2022). The manabí and esmeraldas-borbón forearc basins of ecuador.
- Castagna, J. P. and Backus, M. M. (1993). *Offset-dependent reflectivity—Theory and practice of AVO analysis*. Society of Exploration Geophysicists.

- Catuneanu, O. and Eriksson, P. G. (2007). Sequence stratigraphy of the precambrian. *Gondwana Research*, 12:560–565.
- Closs, M. (1993). Lithospheric buoyancy and collisional orogenesis: Subduction of oceanic plateaus, continental margins, island arcs, spreading ridges, and seamounts. *Geological Society of America Bulletin*.
- Daly, M. C. (1989). Correlations between nazca/farallon plate kinematics and forearc basin evolution in ecuador.
- Deniaud, Y. (2000). *Enregistrement sédimentaire et structural de l'évolution géodynamique des Andes Equatoriennes au cours du Néogène: étude des bassins d'avantarc et bilan de masse*. PhD thesis, Université Joseph Fourier.
- Evans, C. D. R. and Whittaker, J. E. (1982). The geology of the western part of the borbón basin, north-west ecuador.
- Faust, L. (1951). *Seismic velocity as a function of depth and geologic time*. Geophysics.
- Gallagher, K. and Lambeck, K. (1989). Subsidence, sedimentation and sea-level changes in the eromanga basin, australia. *Basin Research*, 2(2):115–131.
- Galvez, G. and Gutierrez, M. (2005). Interpretación geológica a partir de imágenes satelitales y fotografías aéreas del plan nacional de sistema de información geográfica – dinage de las hojas geológicas río verde (41), valdez (61) y s.n. (60).
- Goonses, P. and Rose, W. (1973). Chemical composition and age determination of the tholeitic rocks in the basic igneous complex, ecuador. *GSA Bulletin*.
- Haq, B. U., Hardenbol, J., and Vail, P. R. (1987). Chronology of fluctuating sea levels since the triassic.
- Hessler, A. and Harman, G. (2018). Subduction zones and their hydrocarbon systems. *Geosphere*.
- Horton, B. K. (2018). Sedimentary record of andean mountain building. *Earth Sci. Rev.*

- Jaillard, E., Benitez, S., and MASSLE, G. H. (1997). Les déformations paléogènes de la zone d'avant-arc sud-equatorienne en relation avec l'évolution géodynamique. *Bull Soc Geol.*
- Jaillard, E. and Soler, P. (1996). Cretaceous to early paleogene tectonic evolution of the northern central andes (0–18°s) and its relations to geodynamics. *Tectonophysics*, 259:41–53.
- Jarrin, A. (1974). Exploration and development of new hydrocarbon resources in pacific basins of ecuador: Abstract.
- Kazemeini, S., Fomel, S., and Juhlin, C. (2008). Prestack spectral blueing: A tool for increasing seismic resolution. *Seg Technical Program Expanded Abstracts*, 27:854–858.
- Kearey, P., Klepeis, K., and Vine, F. (2009). Global tectonics. *John Wiley Sons.*
- Kerr, A. C., Aspden, J. A., Tarney, J., and Pilatasig, L. F. (2002). The nature and provenance of accreted oceanic terranes in western ecuador: Geochemical and tectonic constraints. *Journal of the Geological Society*, 159:577–594.
- Lara-Gonzalo, A., Morato, A., Escobar, M., Guzman, M., Lopez, P., Márquez, G., and Lorenzo, E. (2019). Origin of crude oils from southern coastal ecuador: A case study of quantitative extended diamondoid analysis (qeda). *29th International Meeting on Organic Geochemistry.*
- Lebrat, M., Mégard, F., Dupuy, C., and Dostal, J. (1987). Geochemistry and tectonics setting of pre-collision cretaceous and paleogene volcanics rocks of ecuador. *Geological Society of America Bulletin*, 99:569–578.
- Lonsdale, P. (2005). Creation of the cocos and nazca plates by fission of the farallon plate. *Tectonophysics*, 404:237–264.
- Luzieux, L. (2007). Origin and late cretaceous-tertiary evolution of the ecuadorian forearc. *ETH zurich.*

- Marcaillou, B. and Collot, J. Y. (2008). Chronostratigraphy and tectonic deformation of the north ecuadorian–south colombian offshore manglares forearc basin. *Marine Geology*, 255(1-2):30–44.
- Mégard, F. (1984). The andean orogenic period and its major structures in central and northern peru. *Journal of the Geological Society*, 141:893–900.
- Ming-xiang, M. (2011). Understanding the birth of sequence stratigraphy through the complex geological meanings of unconformity:the first important scientific problem in sequence stratigraphy. *Journal of stratigraphy*.
- Noblet, C., Lavenu, A., and Marocco, R. (1996). Concept of continuum as opposed to periodic tectonism in the andes. *Tectonophysics*, 255:65–78.
- Nygren, W. (1950). Bolivar geosyncline of northwestern south america. *American Association of Petroleum Geologists (AAPG)*.
- Olsson, A. A. et al. (1942). Tertiary and quaternary fossils from the burica peninsula of panama and costa rica.
- Ordoñez, M., Jiménez, N., and Suárez, J. (2006). *MICROPALAEONTOLOGÍA ECUATORIANA " DATOS BIOESTRATIGRÁFICOS Y PALEOECOLÓGICOS DE LAS CUENCAS: GRABEN DE JAMBELÍ, PROGRESO, MANABÍ, ESMERALDAS Y ORIENTE; DEL LEVANTAMIENTO DE LA PENÍNSULA DE SANTA ELENA, Y DE LAS CORDILLERAS CHONGÓN COLONCHE, COSTERA Y OCCIDENTAL*. PETRO-PRODUCCIÓN, CIGG.
- Ramírez, M. (2013). *Registros de la deformación y del volcanismo en el dominio del antearco ecuatoriano: sedimentología y bioestratigrafía de la Formación Borbón*. PhD thesis, Faculty of Engineering in Earth Sciences, ESPOL. Guayaquil.
- Reyes, P. and Michaud, F. (2012). Mapa geológica de la margen costera ecuatoriana. Escala 1:500000.
- Savoyat, F., Vernet, R., Sigal, J., Mosquera, C., Granja, J., and Guevara, G. (1970).

Formaciones sedimentarias de la sierra tectónica andina del Ecuador. *Servicio Nacional de Geología y Minería—Institut Français du Pétrole*.

Spikings, R., Winkler, W., Seward, D., and Handler, R. (2001a). Along-strike variations in the thermal and tectonic response of the continental Ecuadorian Andes to the collision with heterogeneous oceanic crust. *Earth and Planetary Science Letters*.

Spikings, R., Winkler, W., Seward, D., and Handler, R. (2001b). Along-strike variations in the thermal and tectonic response of the continental Ecuadorian Andes to the collision with heterogeneous oceanic crust. *Earth and Planetary Science Letters*, 186:57–73.

Steckler, M. and Watts, A. (1978). Subsidence of the Atlantic-type continental margin off New York. *Earth and Planetary Science Letters*, 41(1):1–13.

Tamay Granda, J. V. et al. (2018). Estructura de cuencas intramontañosas del sur de Ecuador en relación con la tectónica de la cordillera de los Andes a partir de datos geofísicos y geológicos.

Vallejo, C., Spikings, R. A., Horton, B. K., Luzieux, L., Thomsen, T. B., and Winkler, W. (2019). Late Cretaceous to Miocene stratigraphy and provenance of the coastal forearc and western cordillera of Ecuador: Evidence for accretion of a single oceanic plateau fragment.

Weimer, R. J. (1993). Sequence stratigraphy - a historical perspective. *AAPG Bulletin*, 77.

Yilmaz, Ö. (2001). *Seismic data analysis: Processing, inversion, and interpretation of seismic data*. Society of Exploration Geophysicists.

Zhu, W., Mousavi, S., and Beroza, G. (2018). Seismic signal denoising and decomposition using deep neural networks. *IEEE Transactions on Geoscience and Remote Sensing*, 57:9476–9488.

Appendices

.1 Appendix 1.

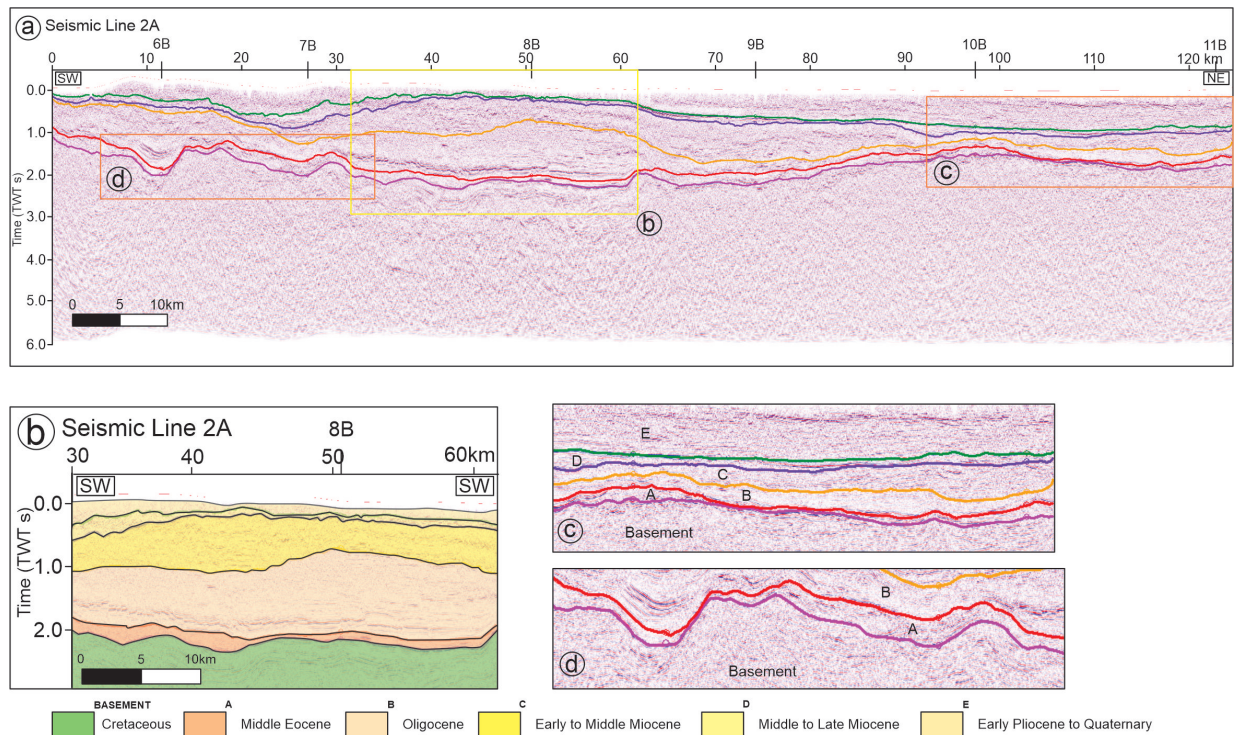


Figure 1: a) Seismic Line A2 (location in Figure 1.1); b) a segment of Seismic Line A3 selected for constructing stratigraphic sequences, highlighting representative reflectors within each sequence to illustrate their geometry—the (location of this segment is marked by a yellow box); c), and d) present detailed views of the seismic profile from Seismic Line 3A (detailed section is identified by orange boxes).